UNIVERSITATEA POLITEHNICA DIN BUCUREŞTI
FACULTATEA ŞTIINŢA ŞI INGINERIA MATERIALELOR

Author: Ing. Dionisie ISTRATE

DOCTORAL THESIS

ABSTRACT

HEAT TREATMENTS INFLUENCE ON THE PERFORMANCE OF AN ALLOY FROM AL-MG SYSTEM FOR MARINE APPLICATIONS

Doctoral supervisors:
Prof. habil. dr. ing. Brânduşa GHIBAN
Prof.dr.ing. Ilare BORDEAŞU

DOCTORAL COMMITTEE

President	**Prof.dr.ing. Cristian PREDESCU**	**de la**	**Universitatea Politehnica din Bucureşti**
Doctoral supervisors	**Prof.habil.dr.ing. Brânduşa GHIBAN**	**de la**	**Universitatea Politehnica din Bucureşti**
	Prof.dr.ing-. Ilare BORDEAŞU	**de la**	**Universitatea Politehnica din Timişoara**
Member	**Prof.dr.ing. Cătălin POPA**	**de la**	**Universitatea Tehnica din Cluj Napoca**
Member	**Prof.dr.ing. Teodor MACHEDON PISU**	**de la**	**Universitatea transilvania Braşov**
Member	**Prof.habil.dr.ing. Iulian Vasile ANTONIAC**	**de la**	**Universitatea Politehnica din Bucureşti**

Bucharest 2023

Content

Chapter 1.....15
The current stage of development of Al-Mg series aluminum alloys.....15
1.1 Introduction …….....15
1.2 The main physical and technological properties of aluminum.....……..….....17
1.3 Aluminum alloys …….....19
1.4 Al-Mg series aluminum alloys.....…….…..…...22
Chapter 2-.....24
Cavitation erosion.....24
2.1 Actual state of knowledge of cavitational erosion ……....…….....….24
2.2 Cavitation erosion behavior of aluminum alloys …….....27
Chapter 3- 29
The research material and methodology used 29
3.1 Research material …….....29
3.2 Investigation methods used in research ……....…….....33
3.3 Methods for investigating the cavitation attack behavior of Al-Mg alloy 36
Chapter 4 43
The mechanical and structural behavior of the cast Al-Mg series aluminum alloy used in our own experiments 43
4.1 Determination of the mechanical behavior of the Al-Mg alloy in the cast state 43
4.2 Structural analysis of the experimental Al-Mg alloy …….....…….....50
4.3 Qualitative phase analysis by X-ray diffraction. …….....….64
4.4 Determination of the cavitational erosion behavior of the experimental specimens. Experimental results regarding the determination of MDER. …….....66
4.5 Macro and microstructural analysis of Al-Mg alloy specimens, as cast, subjected to cavitational erosion …….....….74
4.6 Scanning electron microscope analysis …….....….92
4.7 Discussions and interpretations of the results regarding the behavior of the experimental alloy in the as-cast state to cavitational erosion …….....….96
Chapter 5 99
The mechanical and structural behavior of the laminated aluminum alloy Al-Mg series used in our own experiments 99
5.1 Determination of the mechanical behavior of the Al-Mg alloy in the rolled state 99
5.2. Structural analysis of the Al-Mg alloy …….....106
5.3 Qualitative phase analysis by X-ray diffraction …….....109
5.4 Determination of the cavitational erosion behavior of the experimental specimens. Experimental results regarding the determination of MDER …….....……...……111
5.5 Macro and microstructural analysis of Al-Mg alloy specimens, rolled condition, subjected to cavitation erosion …….....……118
5.6 Scanning electron microscope analysis …….....……....……..131
5.7 Discussions and interpretations of the results regarding the behavior of the experimental alloy in the rolled state to cavitational erosion …….....……..…136
Chapter 6 139
Conclusions and original contributions of the research undertaken within the present paper.

Directions and perspectives of future experimental research 139
6.1 Conlusions 139
6.2 Original contributions 143
6.3 Directions and perspectives of future experimental research 145
Bibliography 148

Chapter 1- entitled *Current status of development of Al-Mg series aluminium alloys*, consists of four sub-chapters as follows: introduction to the current status of aluminium alloys (with definition of main applications); main physical and technological properties of aluminium; main types of alloys according to the Aluminium Association and the American National Standards Institute, and presentation of the main types of Al-Mg series alloys**.**

Chapter 2- entitled *Cavitational erosion*, consists of two sub-chapters, as follows: the current state of knowledge of cavitational erosion and the cavitational erosion behaviour of aluminium alloys. At the end of the chapter the objectives of the present doctoral thesis are presented, respectively:

- Determination of the cavitational erosion resistance of Al-Mg alloy in both cast and plastic deformed (rolled) state after application of different heat treatments.
- Highlighting different possibilities to improve the mechanical characteristics of Al-Mg aluminium alloy by applying homogenisation heat treatments at different temperatures and holding times and ageing treatment at different temperatures and stabilizing times.
- To establish a possible correlation between the structure of Al-Mg alloy (in different structural states, i.e. cast and plastically deformed), mechanical characteristics and resistance to cavitational erosion.

Chapter 3- entitled *Material and research methodology used*, consists of four sub-chapters. The research material consisted of specimens taken from the Color Metal company of various aluminium alloy blanks of the 5000 series, respectively Al-Mg, in two structural states: cast state and rolled state (H111). The chemical composition according to EN 573-3:2019 of the investigated alloy Al-Mg is illustrated in Tab.1a in cast state and Tab. 1b in rolled state.

Tab. 1a- Chemical composition of experimental alloy specimens Al-Mg, cast

Sample	Chemical Composition, % Rate								
	Si	Fe	Cu	Mn	Mg	Cr	Zn	Ti	Al
Experimental	0,41	0,29	0,106	0,52	4,21	0,12	0,16	0,028	Rest
SR EN 373- 3	Max 0,40	Max 0,40	Max 0,10	0,4-1,0	4,0-4,9	0,05-0,25	Max 0,25	Max 0,15	Rest

Tab. 1b- Chemical composition of experimental alloy specimens Al-Mg, rolled

Sample	Chemical Composition, % Rate								
	Si	Fe	Cu	Mn	Mg	Cr	Zn	Ti	Al
Experimental	0.38	0,36	0,052	0,49	4,59	0,06	0,045	0.01	Rest
SR EN 373- 3	Max 0,40	Max 0,40	Max 0,10	0,4-1,0	4,0-4,9	0,05-0,25	Max 0,25	Max 0,15	Rest

The following heat treatments were carried out on the initial blanks in order to increase the mechanical performance and possibly the resistance to cavitational erosion:

Homogenization treatments were applied to the cast specimens at:

- 350°C/100 min / air/ followed by artificial ageing at 180°C / 1h, 12h, 24h;
- 450°C/100 min / air/ followed by artificial ageing at 140°C / 1h, 12h, 24h
- 450°C/100 min / air/ followed by artificial ageing at 180°C / 1h, 12h, 24h

Artificial ageing treatments were applied to specimens in the rolled state (H111 , homogenisation at 455 °C/rolled from 454 °C to 399 °C/annealed at 343 °C, followed by air cooling) at:

- 140°C / 1h, 12h, 24h
- 180°C / 1h, 12h, 24h

Each sample has been assigned an identification code according to Tab. 2.

Tab. 2 Identification of samples

Series/ Aliaj	Sample code	Heat treatment for homogenisation and artificial ageing (T6)
5000 /Al-Mg	**H**	**Gauge sample -cast**
	HAP	la 350°C / stabilizing 100 min / cooling air still followed by artificial aging at 180°C / 1h,
	HAL	la 350°C / stabilizing 100 min / cooling air still followed by artificial aging at 180°C / 12h,
	HAI	la 350°C / stabilizing 100 min / cooling air still followed by artificial aging at 180°C / 24h,
	HNOP	la 450°C/ stabilizing 100 min / cooling air still followed by artificial aging at 140°C / 1h,
	HNOL	la 450°C / stabilizing 100 min / cooling air still followed by artificial aging at 140°C / 12h,
	HNOI	la 450°C / stabilizing 100 min / cooling air still followed by artificial aging at 140°C / 24h,
	HNP	la 450°C / stabilizing 100 min / cooling air still followed by artificial aging at 180°C / 1h,
	HNL	la 450°C / stabilizing 100 min / cooling air still followed by artificial aging at 180°C / 12h,
	HNI	la 450°C / stabilizing 100 min / cooling air still followed by artificial aging at 180°C / 24h,
	X	**Gauge sample - roll down, state H111**
	XOP	artificial ageing at 140°C / 1h,
	XOL	artificial ageing at 140°C / 12h,
	XOI	artificial ageing at 140°C / 24h,
	XP	artificial ageing at 180°C / 1h,
	XL	artificial ageing at 180°C / 12h,
	XI	artificial ageing at 180°C / 24h,

The homogenization and artificial ageing heat treatments were carried out at the Polytechnic University of Bucharest, Faculty of Materials Science and Engineering, according to the cycle diagram Fig. 3.3 using the Thermo SCIENTIFIC-THERMOLYNE oven type heat treatment furnace, shown in Fig. 1

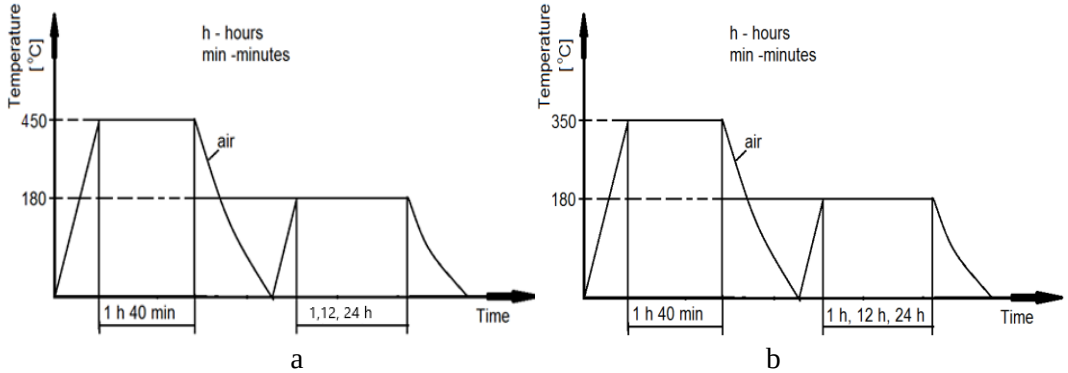

Fig. 1. Heat treatment cycle; a-at 450°C, b- at 350°C

Investigation methods used in the research were: stereomicroscope analysis, optical microscopy, scanning electron microscopy and X-ray diffraction analysis, and methods to investigate the behaviour under cavitational attack.

The experimental program is shown in Fig. 2.

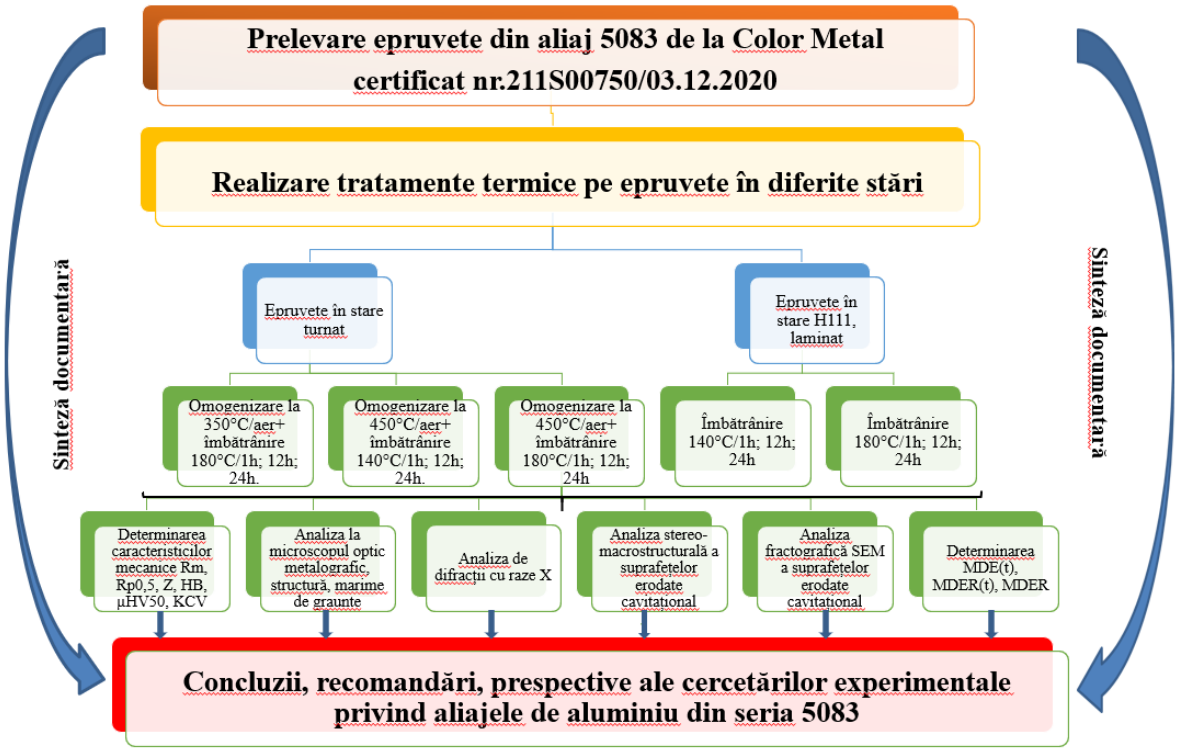

Fig. 2 - Experimental research programme of the present work

Chapter 4 is entitled *Mechanical and structural behaviour of cast Al-Mg series aluminium alloy used in own experiments*. In the first sub-chapter the mechanical behaviour of Al-Mg alloy in cast condition is reported. The analysis of the evolution of the values of the comparative mechanical characteristics for each individual specimen is shown in sequence in **Fig. 3 ÷ Fig. 7**.

From the graph in **Fig. 3a** and **Fig. 3b** it can be seen that the values of the tensile strength increase significantly by applying the heat treatment. After homogenization and ageing at 180^0C, at different holding times, the highest values are obtained, i.e. 318 MPa for 1h holding (31% higher than the value of the control sample), followed by 346.20 MPa, at 12h holding, (37% increase) and the highest value after 24h, i.e. 436 MPa (approximately 50% increase). By applying the homogenization treatment at 450^0C the values of the breaking strength are higher than those of the control sample, but do not reach those of a homogenization at 350^0C, regardless of the type of ageing applied. By applying the heat treatment of homogenisation at 450^0C followed by ageing at 140^0C, values higher than the control sample are obtained by about 25% (at 1h holding), about 28% (at 12h holding) and about 30% (at 24h holding). Values close to those of homogenization at 450^0C + 140^0C are also obtained for homogenization at 450^0C + 180^0C, slightly increased at longer holding times, respectively 30% (at 12h) and 31% (at 24h). **Fig.4** shows the evolution of the yield strength values, from which it can be seen that the highest values are obtained by homogenization at 350^0C + aging at 180^0C. Increasing the aging time has a dramatic effect. After 1 hour, the yield strength increases by about 21% (compared to the control sample), after 12 hours it increases by 40%, and after 24 hours the yield strength increases by 67%. On the other hand, by applying homogenisation at 450^0C and ageing (either at 140^0C or 180^0C), the yield strength increases at much lower rates than the control sample, i.e. by (14 ÷ 18)% for 1400C and (19 ÷ 25)% for 180^0C.

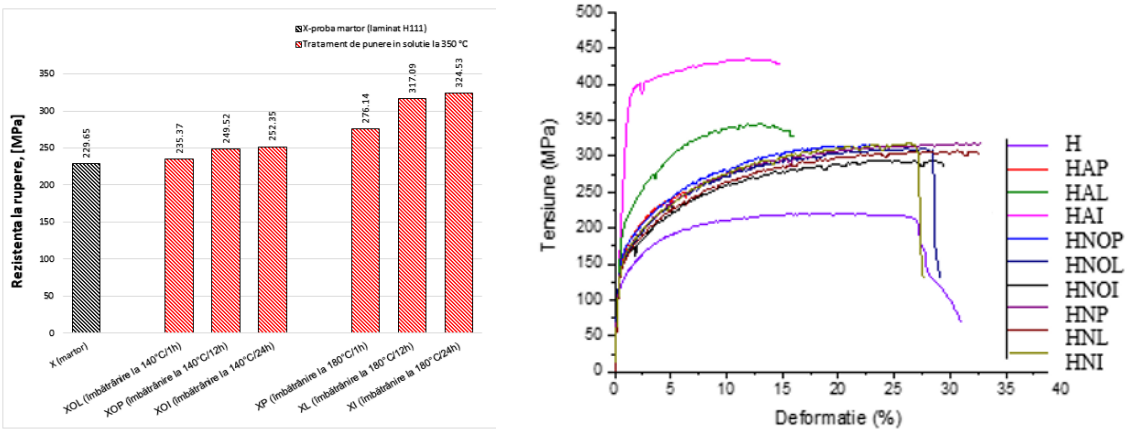

a b

Fig. 3. - Evolution of the tensile strength values of experimental Al-Mg alloy specimens, in the tuned state, in different structural states (a) and stress-strain curves of Al-Mg alloy specimens, in the cast state (b)

The variation of elongation values of experimental samples is shown in **Fig. 5**. The applied heat treatments lead to a decrease of the elongation values from 28.4% to (control sample), halving the different ageings. At homogenization at 350^{0}C the decrease in elongation values is intermediate, from 66% (for ageing at 180^{0}C/1h), to 92% (180^{0}C/ 12h) and 123% (at 180^{0}C/24h). The highest elongation values after ageing are obtained at 450^{0}C / +140^{0}C. Thus, the decreases in elongation values are lower by about 21% (for 1h), followed by 34% (at 12h) and 48% (at 24h). Values similar to those obtained for homogenisations at 350^{0}C + 180^{0}C were obtained for samples homogenised at 450^{0}C + 180^{0}C. The variation of the resilience values of the experimental specimens is shown in **Fig. 6.** By applying the heat treatment of homogenisation plus ageing, in addition to the homogenisation of the grain size, a change in the resilience occurs leading to decreases below 25J/cm2 , values not acceptable for further applications. It can be judged that homogenisation at 350^{0}C + 180^{0}C, regardless of the duration of ageing maintenance, does not take the material out of the parameters, the resilience reaching the accepted limit value of 25.2 J / cm2 (at 24h maintenance). The same is not true for homogenisations at 450^{0}C followed by ageing. If at 450^{0}C + 140^{0}C increasing the ageing time leads to drastic decreases in resilience (22 J/cm2 at 12h, respectively 18 J/cm2 at 24h), at 180^{0}C ageing only the 24h holding takes the material out of the parameters, reaching 18 J/cm2, at the other ageing times the resilience values remain high (31 J/cm2 and 17 J/cm2 respectively). The evolution of the hardness values of the experimental specimens is shown in **Fig. 7**. Compared to the hardness of the control specimen, i.e. 79.8 MPa, through homogenisation and ageing the hardness values decrease. After homogenization at 350^{0}C + 180^{0}C there is an average decrease of about 1 ÷ 4%, at 450^{0}C + 140^{0}C there is a decrease of 4 ÷ 9%, and for 450^{0}C + 180^{0}C / 1h there is the largest decrease, i.e. 10%. In Tab. 3 the mechanical results of the tested samples are centralized.

The experimental results on grain size determination are shown in **Fig. 8**. It can be seen that in the control sample the average grain size is at the highest level, around 243μm. By applying the heat treatments the grain size decrease occurs. During hardening and ageing at 350^{0}C + 180^{0}C the average grain size is generally larger than at 450^{0}C + 180^{0}C or 450^{0}C + 140^{0}C. The plot of grain size variation as a function of the heat treatment applied to the experimental samples is shown in **Fig. 9**.

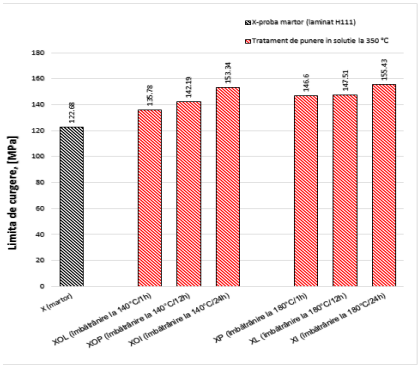

Fig. 4. Evolution of the yield strength values of experimental Al-Mg alloy samples in the cast state in different structural states.

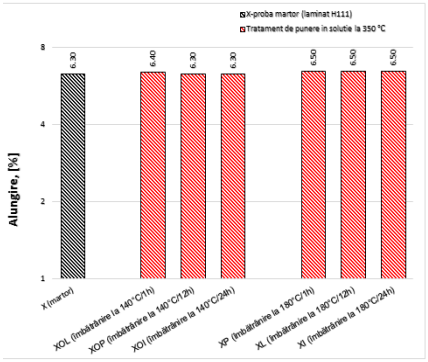

Fig. 5. Evolution of elongation values of experimental Al-Mg alloy samples, in the cast state, in different structural states

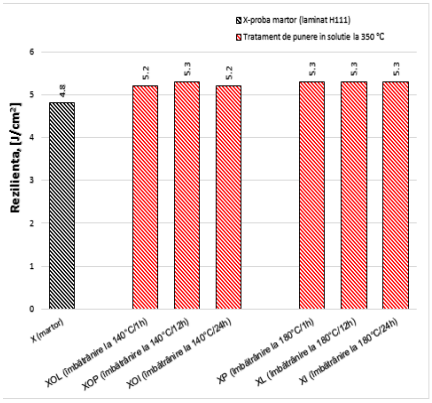

Fig. 6. Evolution of the resilience strength values of experimental Al-Mg alloy samples in the cast state in different structural states

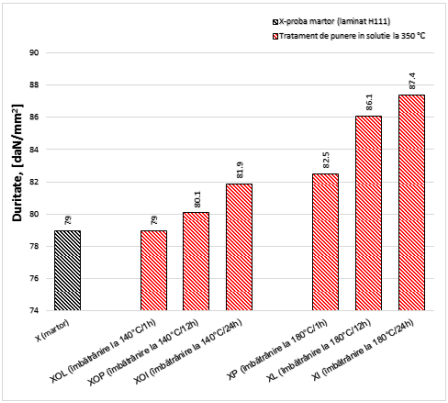

Fig. 7. Evolution of hardness values of experimental Al-Mg alloy samples in the cast state in different structural states

Tab. 3. Mechanical behavior and grain size of the experimental samples type Al-Mg in different structural states.

Sample code	State	Mechanical Characteristics					
		Yielding Strength [MPa]	Ultimate strength [MPa]	Ductility [%]	Brinell Hardness [MPa]	Vickers Hardnes µHV	Impact Toughness [J/cm^2]
H	Gauge sample	118.84	220.63	28.40	79.80	76.97	32.00
HAP	350°C / 100 min / air + 180°C / 1h	151.21	318.58	17.11	76.80	76.89	31.00
HAL	350°C / 100 min / air + 180°C / 12h	195.70	346.20	14.75	79.00	79.14	25.80
HAI	350°C / 100 min / air + 180°C / 24h	356.68	436.30	12.73	79.00	80.01	25.20
HNOP	450°C / 100 min / air + 140°C / 1h	139.57	294.82	23.44	72.80	74.65	32.60
HNOL	450°C / 100 min / air + 140°C / 12h	141.66	307.63	21.17	76.80	75.30	22.10
HNOI	450°C / 100 min / air + 140°C / 24h	144.55	311.21	19.18	76.80	80.67	18.00
HNP	450°C / 100 min / air r + 180°C / 1h	146.50	250.03	12.68	71.80	78.12	31.70
HNL	450°C / 100 min / air + 180°C / 12h	149.91	315.16	13.18	77.90	78.38	28.40
HNI	50°C / 100 min / air + 180°C / 24h	158.62	318.34	14.44	80.70	79.68	16.40

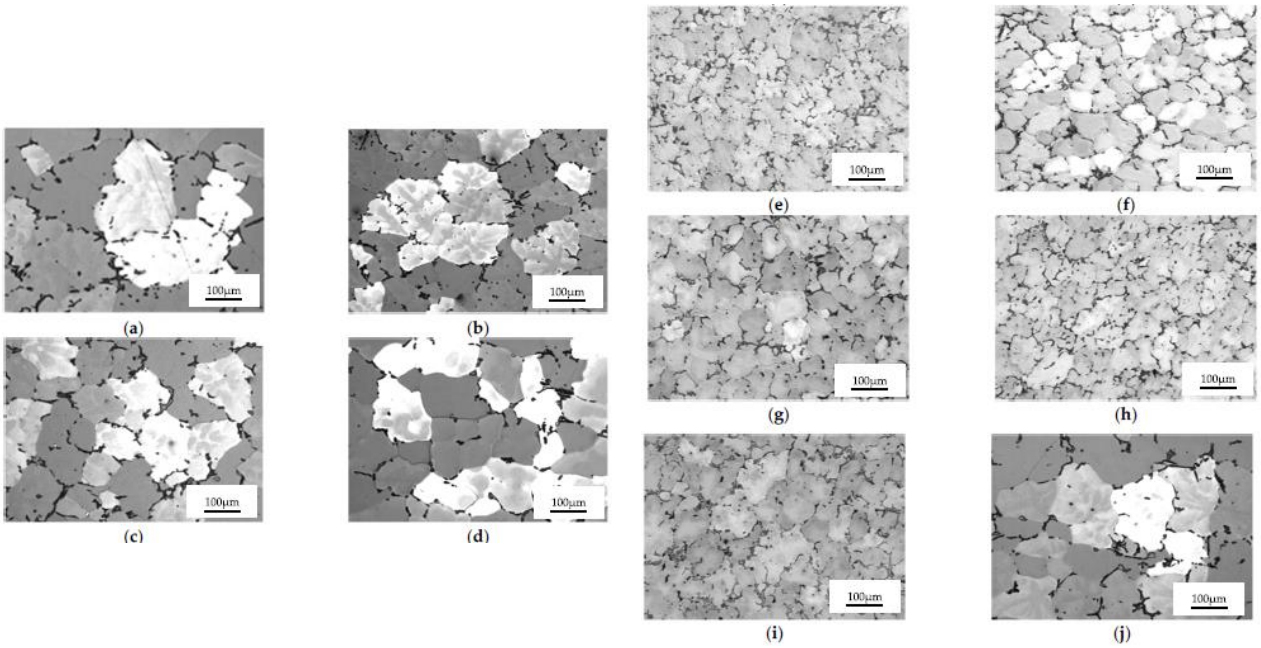

Fig. 8 Structural analysis of Al-Mg aluminium alloy experimental samples in the cast state: control sample (H); (b, c, d)- cast + homogenization at 350℃ / 100 min / air + artificial ageing at 180℃; (e, f, g) cast + homogenization at 450℃ / 100 min air + artificial ageing 140℃; (h, i, j) cast + homogenization at 450℃ / 100 min / air + artificial ageing at 140℃; Holding times - (b, e, h- 1h); (c, f, i- 12 h); (d, g, j- 24h)

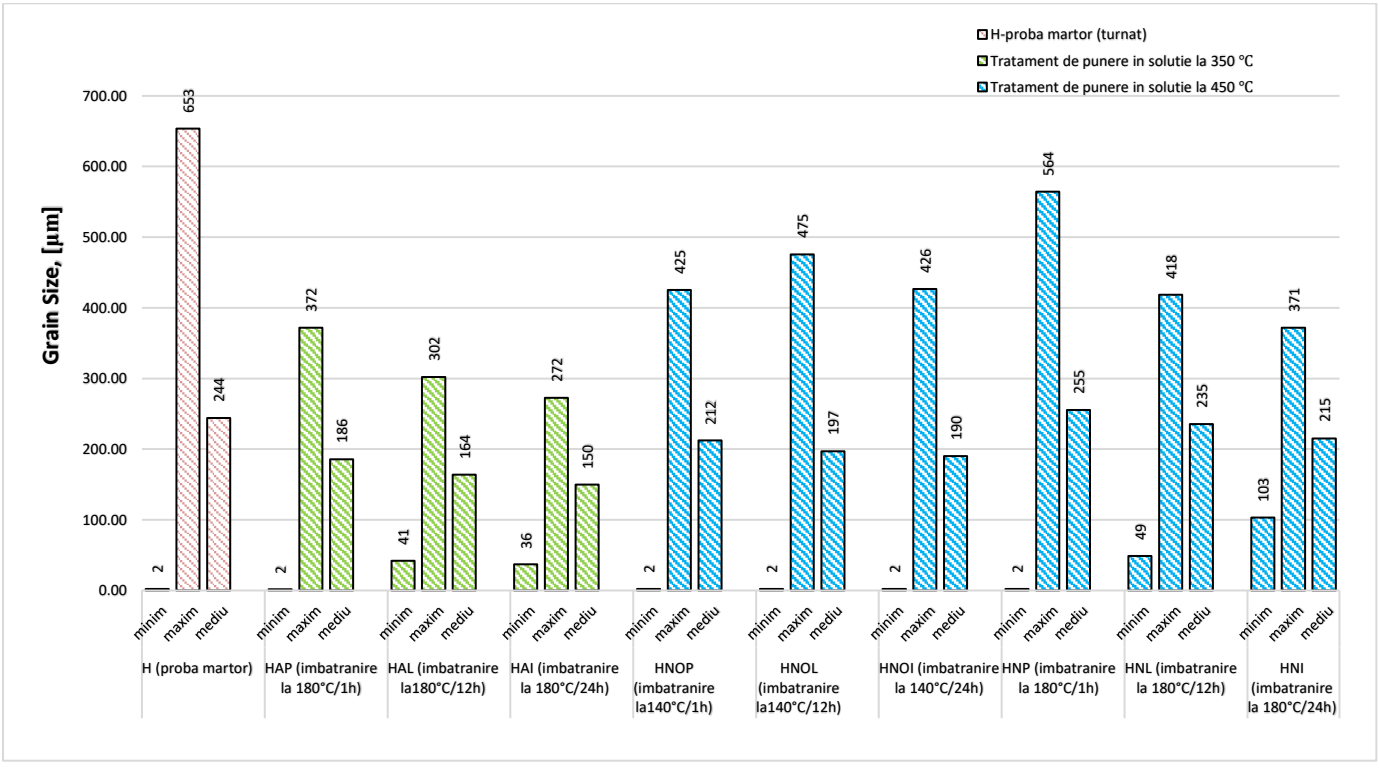

Fig. 9- Grain size histogram of the experimental cast Al-Mg alloy samples, in different structural state.

In the sub-chapter entitled *X-ray diffraction qualitative phase analysis*, the appearance of diffractograms for specimens subjected to different heat treatments is presented, **Fig. 10**. A careful analysis of the values of the elementary cell parameters revealed that the application of the quenching + ageing heat treatments can change this parameter. The combination 450°C +140°C leaves the elementary cell parameter unchanged, i.e. 4.073 [Å], compared to the control sample. In contrast to the other heat treatments there is an increase in the lattice parameter, either in the range 4.072 ÷ 4.075 [Å] when applying the 350°C + 180°C heat treatments, or an increase in the lattice parameter in the range 4.074÷ 4.076 [Å] when applying the 450°C + 180°C heat treatments.

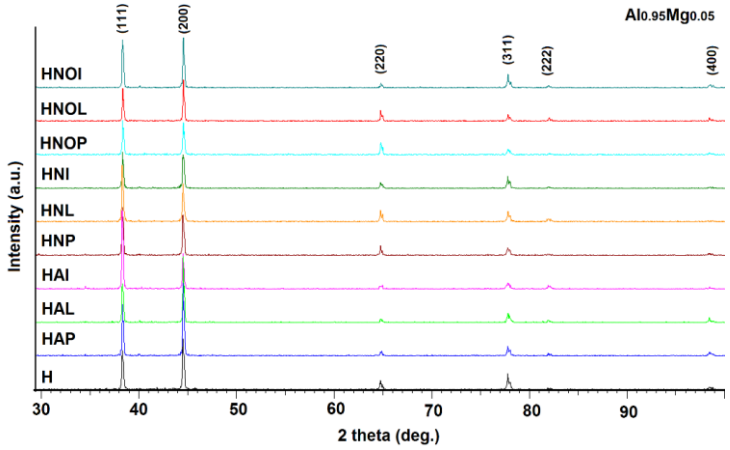

Fig. 10– X-ray diffractograms of cast Al-Mg aluminum alloy samples in different structural states.

In the subchapter entitled *Determination of cavitational erosion behaviour of experimental specimens*, experimental results on the determination of MDER are reported, Fig.11.

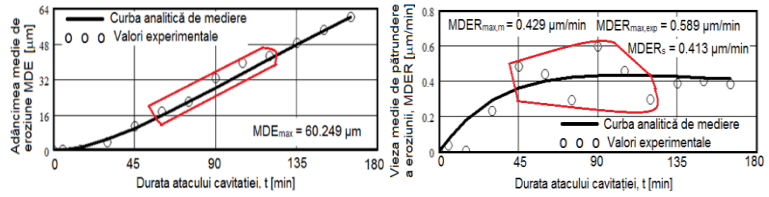

(A = 0,038, B = 0,02)

a b

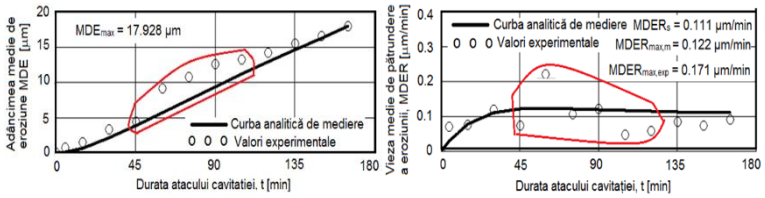

(A = 0,109, B = 0,035)

c d

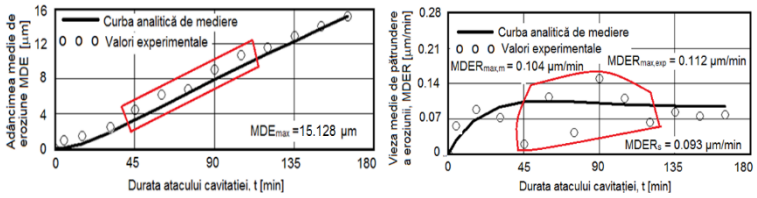

(A = 0,092, B = 0,034)

e f

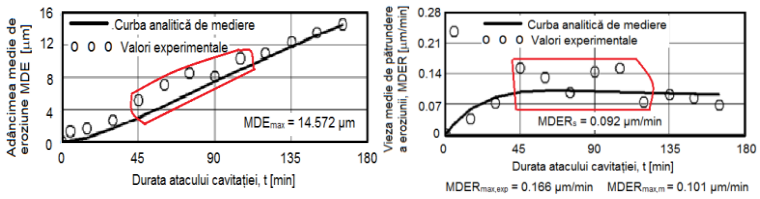

(A =0,089, B = 0,03)

g h

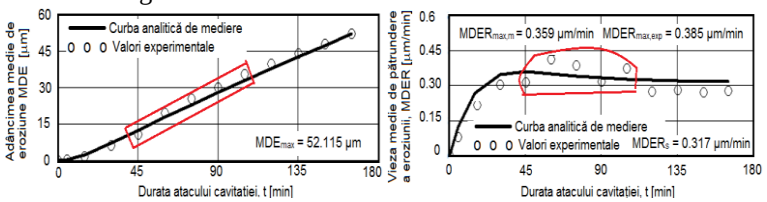

(A = 0,233, B = 0,034)

i j

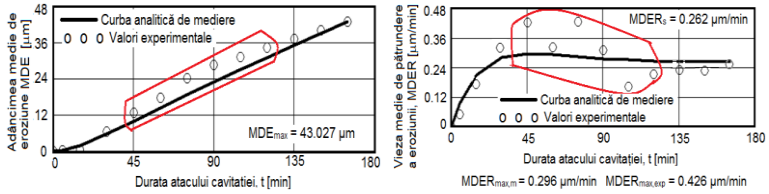

(A = 0,261, B = 0,043)

k l

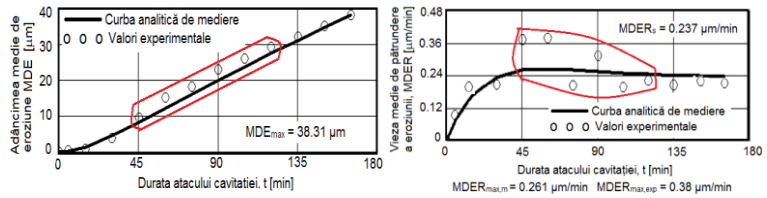

(A = 0,316, B = 0,046)

m n

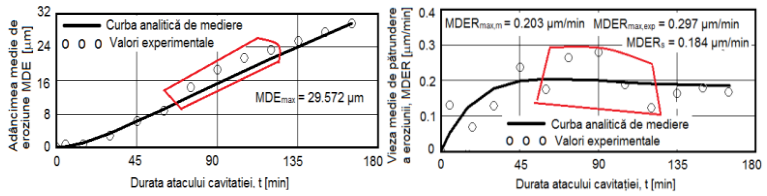

(A = 0,18, B = 0,32)

o p

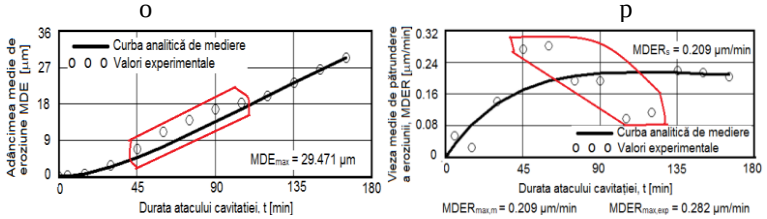

(A = 0,189, B = 0,018)

r s

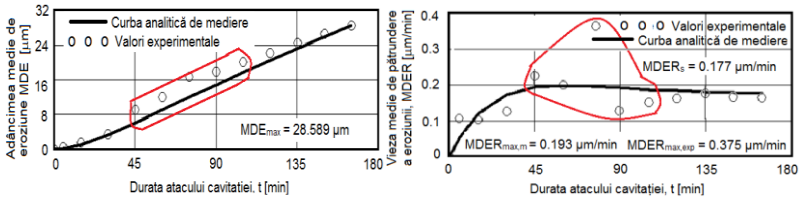

(A = 0,174, B =0,033)

t u

*Fig. 11– Structural analysis of cast experimental samples from aluminum Al-Mg alloy: (**a**) Gauge sample (H), (**b**–**d**) cast + quenched at 350 °C/100 min/air + artificial ageing at 180 °C; (**e**–**g**) cast + quenched at 450 °C/100 min/air + artificial ageing at 140 °C; (**h**–**j**) cast + quenched at 450 °C/100 min/air + artificial ageing at 140 °C (**b**,**e**,**h**) 1 h maintaining, (**c**,**f**,**i**) 12 h maintaining, (**d**,**g**,**j**) 24 h maintaining*

Tab. 4- Erosion-cavitation process parameters of experimental Al-Mg aluminium alloy cast samples

Sample	$MDER_{\max m}$	$MDER_{\max exp}$	$MDER_s$	Δ $\lvert MDER_{\max m} - MDER_{\max exp} \rvert$		Δ $\lvert MDER_{\max m} - MDER_{\max s} \rvert$	
				$\mu m/min$	%	$\mu m/min$	%
H	0.429	0.589	0.413	0.16	37	0.016	5.7
HAP	0.122	0.171	0.111	0.049	40	0.011	9
HAL	0.104	0.112	0.093	0.008	8	0.008	8
HAI	0.101	0.166	0.092	0.065	65	0.009	9
HNOP	0.359	0.385	0.317	0.03	8	0.042	12
HNOL	0.296	0.426	0.262	0.13	44	0.034	12
HNOI	0.261	0.380	0.237	0.109	46	0.014	9
HNP	0.203	0.297	0.184	0.094	46	0.019	10
HNL	0.209	0.282	0.209	0.073	35	0	0
HNI	0.193	0.375	0.177	0.182	95	0.0.16	8

Tab. 5 – Maximum depth of penetration of cavitational attack of cast Al-Mg aluminium alloy specimens in different heat treatment states

Sample	**Maximum penetration depth of the cavitation attack**		
	$MDER_{max}$ (μm)	$\delta_{measured}$ (μm)	$\frac{\delta}{MDER_{max}}$
H	60.249	436.58	7
HAP	17.926	190.01	11
HAL	15.125	162.87	11
HAI	14.572	124.41	8
HNOP	52.115	330.26	6
HNOL	43.027	291.81	7
HNOI	38.31	285.02	7
HNP	29.572	278.23	9
HNL	29.471	262.4	9
HNI	28.589	257.87	9

The following points can be made:

- the most significant losses, with the development of pinpricks and caverns in the exposed surface area are recorded in the interval 45-120 minutes (large differences between successive experimental values of the measured parameters MDE and MDER, as well as large deviations from the MDE(t), and MDER(t) curves) for all experimental specimens;
- in the first 30 minutes an erosive mechanism takes place whereby roughness peaks, abrasive dust and elasto-plastic deformations and crack networks are removed;
- the shape of the approximation/measurement curve of the experimental values has different values between the maximum value (MDERmax) and the one towards which it tends asymptotically towards stabilisation (final MDERs) (as can be seen from Tables 3 and 4, with differences of 0 ÷ 12%. This difference, manifested in all cases, is typical of surfaces with average mechanical properties (with hardness values of about 80 HB and resiliencies of about 25 J/cm^2), which gives this state a behaviour characteristic of metallic materials with low resistance to cavitational erosion;
- if insignificant differences are observed in all heat treatment situations between experimental values of erosion rates after 120 minutes and up to test completion, which lead to an approximately linear increase of the erosion MDE(t) over this time interval and slightly asymptotic towards stabilization of the curve MDER(t) curve, differences characteristic of plastic structures, leading to decrease in the cyclic stress resistance of cavitation microjets;
- a big difference is noticeable (which, as shown in Tab. 4 and Tab. 5, is in the range 8 ÷ 94%) between the maximum value obtained by the experiment (MDER max,exp) and that defined by the averaging curve (MDERmax,m), even if recorded at the same cavitations duration (90 minutes). The smallest difference is for the sample heat-treated at 450°C /100min/air + 140°C /12h/air of about 8%, and the largest difference is for the sample heat-treated at 350°C /100min/air + 180°C /24h/air of about 94%. In the other heat-treated states this difference is in the range 40 ÷ 65%. This is further evidence of the complexity of the mechanics by which the structure responds to cavitational stress and shows the effect of holding time at the ageing heat treatment temperature on the structure and mechanical properties, as a value and mode of distribution in the sample volume.

Cavitational erosion attack images obtained by optical/stereomicroscopic microscope analysis (Fig. 12 ÷ Fig. 15) .

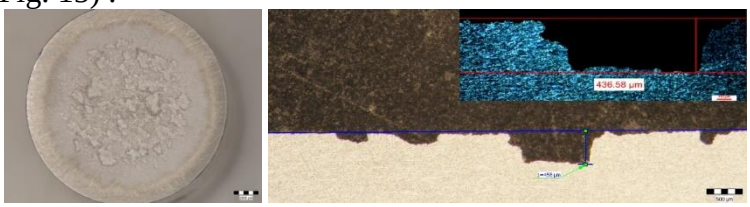

Fig. 12 - Appearance of macrostructural surfaces (left front section, parallel to eroded surface, right in cross section, background - optical microscope image, detail - stereomicroscope image) subjected to cavitational erosion of Al-Mg alloy, in cast condition, control sample.

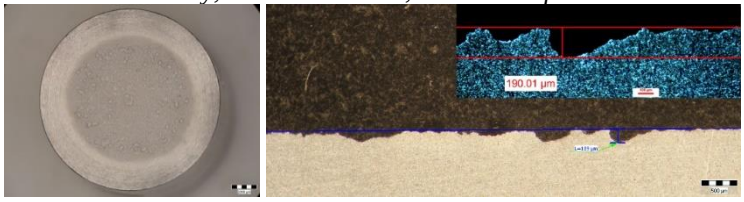

a

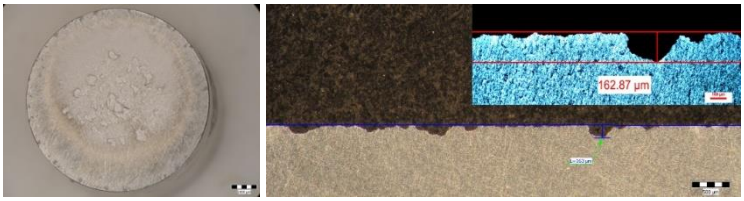

b

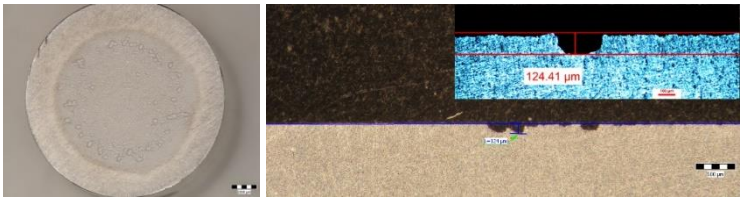

c

Fig. 13- Appearance of macrostructural surfaces (left front section, parallel to eroded surface, right in cross section, background - optical microscope image, detail - stereomicroscope image) subjected to cavitational erosion of Al-Mg alloy, cast followed by solution hardening 350°C / holding 100 min / cooling still air and subjected to artificial ageing at 180°C and different holding times: a- 1h; b- 12h; c- 24 h

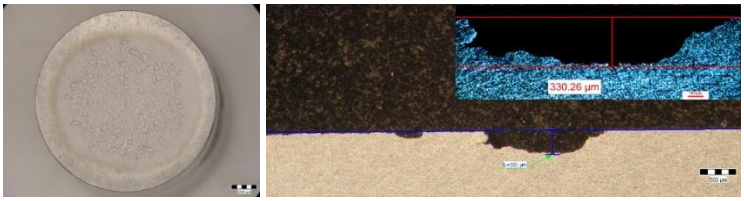

a

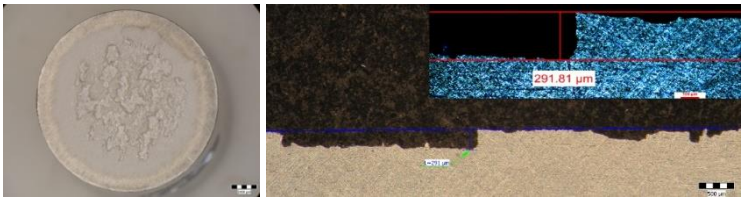

b

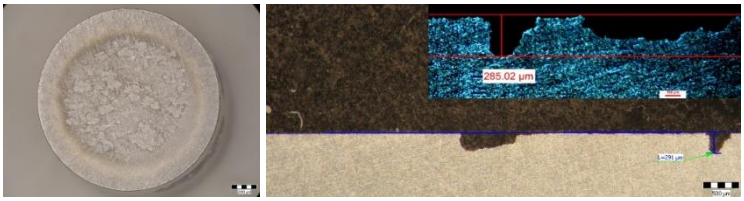

c

Fig. 14- Appearance of macrostructural surfaces (left front section, parallel to eroded surface, right in cross section, background - optical microscope image, detail - stereomicroscope image) subjected to cavitational erosion of Al-Mg alloy, cast followed by solution hardening 450°C / holding 100 min / cooling still air and subjected to artificial ageing at 180°C and different holding times: a- 1h; b- 12h; c- 24 h

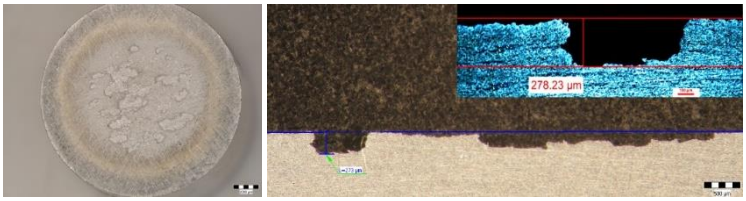

a

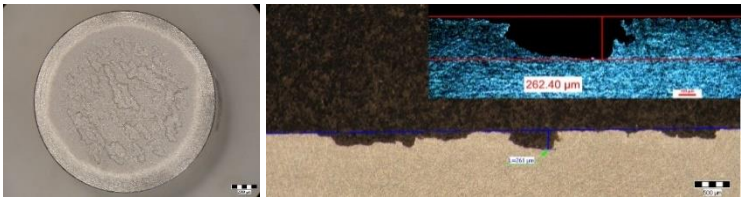

b

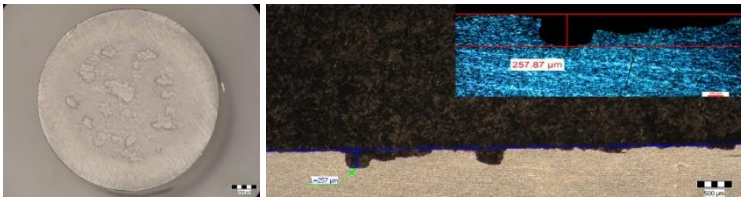

c

Fig. 15-- Appearance of macrostructural surfaces (left front section, parallel to eroded surface, right in cross section, background - optical microscope image, detail - stereomicroscope image) subjected to cavitational erosion of Al-Mg alloy, cast followed by solution hardening 450°C / holding 100 min / cooling still air and subjected to artificial ageing at 140°C and different holding times: a- 1h; b- 12h; c- 24 h

The macrostructural analysis carried out with the stereomicroscope allowed the qualitative and quantitative fractographic analysis of the surfaces subjected to cavitational attack, the results obtained are shown in Tab. 5.

Tab. 6- Stereo macrostructural analysis of Al-Mg alloy specimens, as cast, in the treatment states, required for cavitation attack

Sample code	**Remarks**
H	The region affected by cavitational attack is (10699.0 µm) and with a central area of 7442.0 µm. The area affected by cavitational attack is 71.32%. The central area (the most cavitated area) is 69.62%.
HAP	The region affected by cavitational attack is (10249.3 µm) and with a central area of 9050.7 µm. The area affected by cavitational attack is 68.33%. The central area, (the most cavitated area) is 60.34%.
HAL	The region affected by cavitational attack is (11483.3 µm) and with a central area of 9434.0 µm. The area affected by cavitational attack is 76.55%. The central area (the most cavitated area) is 62.90%.
HAI	The region affected by cavitational attack is (11592.3 µm) and with a central area of 9495.3 µm. The area affected by cavitational attack is 76.86%. The central area (the most cavitated area) is 63.31%.
HNOP	The region affected by cavitational attack is (12039.0 µm) and with a central area of 9048.3 µm. The area affected by cavitational attack is 80.26%. The central area (the most cavitated area) is 60.32%.
HNOL	The region affected by cavitational attack is (12967.3 µm) and with a central area of 10142.0 µm. The area affected by cavitational attack is 68.33%. The central area (the most cavitated area) is 67.61%.
HNOI	The region affected by cavitational attack is (11197.0 µm) and with a central area of 9467.7 µm. The area affected by cavitational attack is 74.64%. The central area (the most cavitated area) is 63.11%.
HNP	The region affected by cavitational attack is (10186.3 µm) and with a central area of 9019.3 µm. The area affected by cavitational attack is 67.90%. The central area (the most cavitated area) is 60.12%.
HNL	The region affected by cavitational attack is (11572.3 µm) and with a central area of 9580.0 µm. The area affected by cavitational attack is 77.15%. The central area (the most cavitated area) is 63.87%.
HNI	The region affected by cavitational attack is (12597.7 µm) and with a central area of 8158.7 µm. The area affected by cavitational attack is 83.99%. The central area (the most cavitated area) is 54.39%.

SEM analysis confirms a brittle behaviour of the Al-Mg alloy after cavitational erosion, the cavitations produced being generated by secondary particles of the alloy, around which the structural integrity is destroyed. Scanning electron microscope (SEM) analysis of the eroded surfaces of Al-Mg alloy specimens, in the cast state (control specimen), at different microscope magnification powers is shown in **Fig. 16** we have SEM analysis of the eroded surfaces of Al-Mg alloy specimens, after rinsing at 350°C / holding 100 min / air-cooled and artificially ageing at 180°C/24h, at different microscope magnification powers:

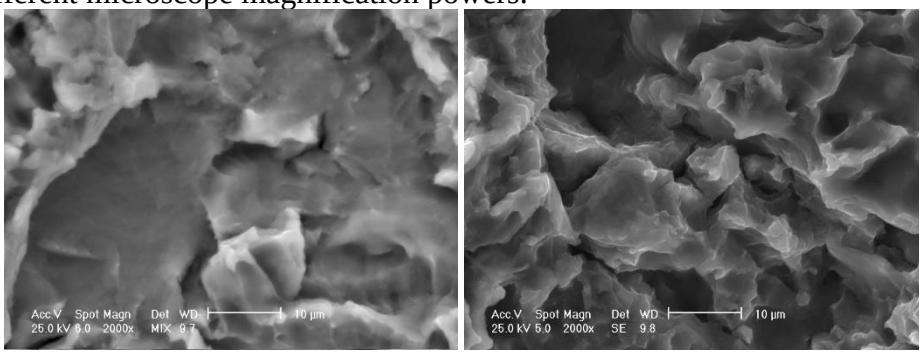

a b

Fig. 16- Scanning electron microscope (SEM) analysis of eroded surfaces of Al-Mg alloy samples, in cast condition (a), and after quenching at 350°C / holding 100 min / air cooled and artificial quenching at 180°C/24h (b)

Comparative analysis of the mechanical behaviour and cavitational erosion behaviour of Al-Mg aluminium alloy samples allows the following interesting observations to be made from the experiments carried out in this thesis. After application of solution quenching at 350 °C/100 min + artificial ageing at 180°Cthe lowest cavitational penetration depths are obtained both with respect to the control sample at 60 μm and with respect to the samples subjected to solution quenching at 450 °C/100 min + artificial ageing (either at 140°C where the range of maximum penetration depths is 38-52 μm, or at 180°C, where the maximum penetration depth is about 29 μm). At the same time, the correlation between the highest values of the mechanical characteristics obtained after solution quenching at 350 °C/100 min + artificial ageing at 180°C (1h, 12h, 24h) and the cavitational erosion behaviour, which is the most favourable for these heat treatments applied to Al-Mg aluminium alloy tuned products, can be noticed. By applying homogenisation heat treatments, either at 350°C or 450°C, followed by artificial ageing (140°C or 180°C), the mechanical and structural characteristics of Al-Mg alloy cast products can be modified. The values of breaking strength and yield strength change similarly. Thus, the highest values of these characteristics are recorded after homogenisation at 350°C + artificial ageing at 180°C/ 24h (mechanical strength values double and yield strength values triple compared to the control sample). Elongation values are intermediate for homogenization at 350°Ccompared to homogenization at 450°C, regardless of the aging time. The resilience values after heat treatment of homogenization at 350°C+ ageing at 180°Cdo not decrease below 25J/cm^2 regardless of the ageing duration. Other heat treatments can lead to drastic decreases in resilience, below 25J/cm^2 (such as after homogenisation heat treatment at 450°C+ 140°C/12h, or 450°C+ 140°C/ 24h). Values hardness values decrease slightly after homogenisation at 350°C + 180°C (only 1-4%), compared to homogenisation at 450°C + 140°C, where hardness decreases up to 10% compared to the control sample. The lowest values of the mean grain size are homogenisations at 350°C + 180°C, average grain sizes at 450°C + 140°C and largest grain sizes at 450°C + 180°C. By applying heat treatments to the products cast Al-Mg alloy, either solution quenching at 350°C/100 min + artificial ageing at 180°C (1h, 12h, 24h) or solution quenching at 450 °C/100 min + artificial ageing at 140°C (1h, 12h, 24h) or solution quenching 450 °C/100 min + artificial ageing at 180°C (1h, 12h, 24h) can increase the resistance to cavitational corrosion in the sense of decreasing the depths and speeds of erosion penetration. Within the same combination

of heat treatments, increasing the retention time for artificial ageing causes the maximum penetration depths of the cavities to decrease. After solution quenching at 350°C /100 min + 180°C (Fig. 4.19 c, d, e, f, g, h) the maximum cavitations penetration depth MDEmax, decreases from 17.928 μm (at 1h holding), to 15.128 μm (at 12h holding), reaching 14.572 μm (at 24h holding). After solution quenching at 450°C /100 min + 140°C (Fig. 4.19 i, j, k, l, m, n) the maximum depth of cavitations MDEmax decreases from 52,115 μm (at 1h holding) to 43,017 μm (at 12h holding) to 38,31 μm (at 24h holding). After solution quenching at 450°C /100 min + 180°C (Fig. 4.19 o, p, r, s, t, u) the maximum depth of cavitations MDEmax decreases from 29,572 μm (at 1h holding) to 29,471 μm (at 12h holding) to 28,589 μm (at 24h holding). The best combination of heat treatments applied to Al-Mg aluminium castings is homogenisation at 350°C followed by artificial ageing at 180°C, at which the best mechanical characteristics are obtained, breaking strength 436. 30 [MPa], yield strength of 356.68 [MPa], hardness of 79.00 [MPa], scratch size of 150 μm and minimum erosion depth MDEmax around 14.572 μm, and the lowest ratio between the diameter of the most affected zone and the initial diameter of the specimen of about 54%.

Chapter 5 is entitled *Mechanical and structural behaviour of rolled Al-Mg series aluminium alloy used in own experiments*. The experimental results on the determination of the mechanical characteristics are successively shown in **Fig. 17 ÷ Fig. 22**. From the graph in **Fig. 17a** it can be seen that the values of the resistance to rupture increase after the ageing process at 180°C at different holding times, the highest values are obtained, i.e. 276 [MPa]for 1h holding (17% higher than the value of the control sample), followed by 317 [MPa] at 12h holding (28% increase) and the highest value after 24h, i.e. 324 [MPa] (approximately 30% increase). From the analysis of the values of the resistance to rupture (**Fig.17**) it can be seen, first of all, that the application of the ageing heat treatment can increase this value by about 17÷30% compared to the value of the control sample. The increase is smaller for ageing at 140°C / 1, 12, 24h (maximum 9%) and more significant for ageing at 180°C / 1, 12, 24h (reaching up to 30%). At the same time, during the same ageing, the holding time also determines the increase in the breaking strength, consequently the highest increase in mechanical strength is recorded after ageing at 180°C / 24h (with an increase of 30% compared to the breaking strength of the sample in the rolled state, the control sample). Similar considerations can be made for the evolution of the yield strength values (**Fig. 18**). Thus, by applying thermal ageing treatment to rolled Al-Mg alloy products, the yield strength can increase by about 10÷21%. When applying ageing heat treatment at 140°C/1, 12, 24h, the maximum increase of the yield strength reaches up to 14%, while after applying ageing heat treatment at 180°C/1, 12h, 24h the increase of the yield strength can reach up to 21%. Consequently, the highest increase of the yield strength is recorded after the application of the artificial ageing heat treatment at 180°C / 24h (increase of about 21% compared to the yield strength of the control sample). These changes in the mechanical characteristics are due to a slight precipitation hardening of the particles inside the metal matrix. The evolution of the elasticity values shown in **Fig. 19** indicates that they are very little influenced by the application of the ageing heat treatment (180°C/24h increase of about 3% compared to the yield strength of the control sample). These values are in the tight range of 6.3 ÷ 6.5%. **Fig. 20** shows the influence of the artificial ageing heat treatment on fracture toughness. Thus the fracture toughness increases by artificial ageing regardless of the temperature value or the holding time by about 9%, the values being in the range 5.2 ÷ 5.3 J/cm^2. In **Fig. 21** it is observed that by performing the artificial ageing heat treatment, only ageing at 180°C / 24h increases the toughness values by about 10%, in all other cases, the toughness increases progressively (1-8%). The analysis of the microhardness values, **Fig. 22**, shows a similar variation of these values to that of the toughness values. Also in this situation, ageing at 180°C/24h results in an increase of Vickers microhardness values of about 10%, in all other situations the increase is

3÷4%. In Tab. 7 the mechanical results of the tested samples are centralized.

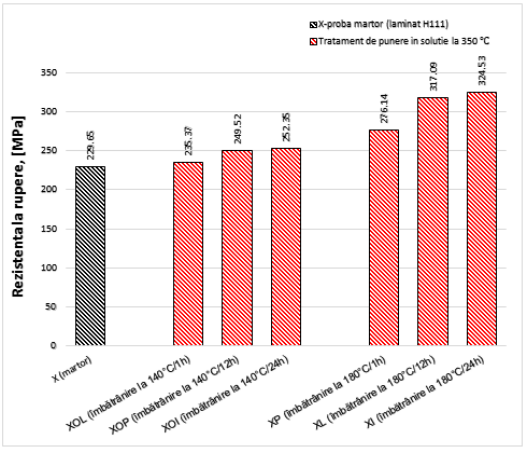

Fig. 17a Ultimate strength experimental values rolled alloy Al-Mg, in different structural states

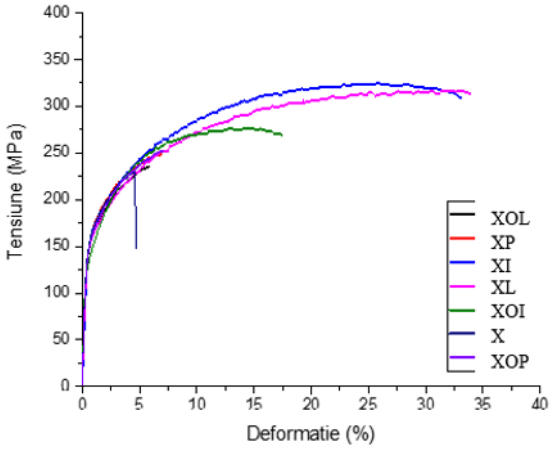

Fig. 17b The stress-strain curves of the Al-Mg alloy specimens, in the rolled state

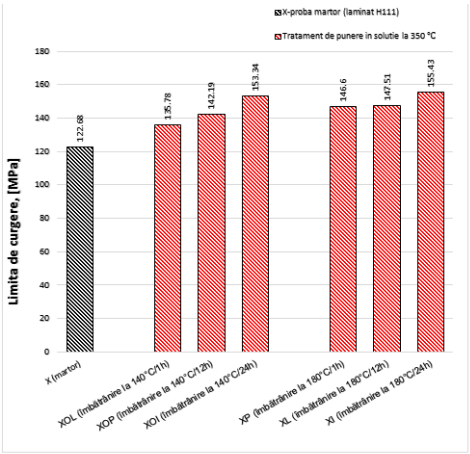

Fig. 18 Evolution of yield strength values of experimental Al-Mg alloy samples, rolled, in different structural states

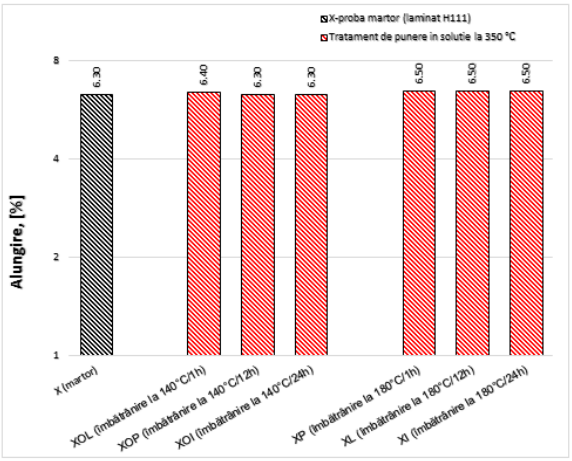

Fig. 19 Ductility values experimental values of rolled alloy Al-Mg, in different structural states

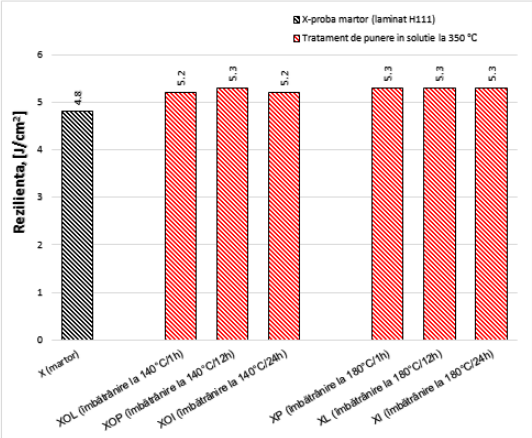

Fig. 20. Impact Toughness experimental values of rolled alloy Al-Mg, in different structural states

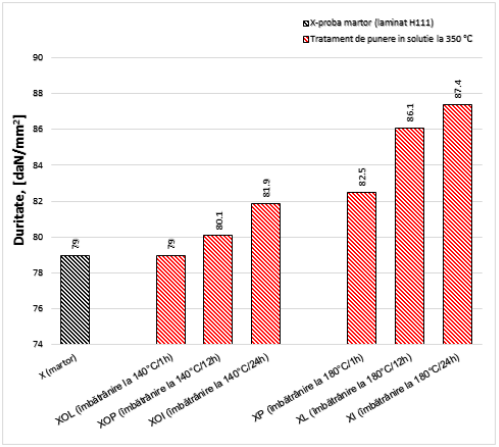

Fig. 21- Brinell Hardness experimental values of rolled alloy Al-Mg, in different structural states

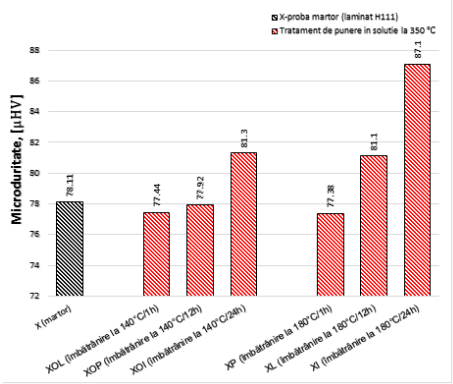

Fig. 22- Vickers hardness experimental values of rolled alloy Al-Mg, in different structural states

Tab. 7. The values of the mechanical characteristics of the experimental samples type Al-Mg in different structural states.

Sample code	State	Mechanical Characteristics					
		Ultimate strength [MPa]	Yielding Strength [MPa]	Ductility [%]	Brinell Hardness [MPa]	Vickers Hardness µHV	Impact Toughness [J/cm^2]
X	Gauge sample	229.65	122.68	6.3	79.0	78.11	4.8
XOP	140°C/ 1h	235.37	135.78	6.4	79.0	77.44	5.2
XOL	140°C/ 12h	249.52	142.19	6.3	80.1	77.92	5.3
XOI	140°C/ 24h	252.35	153.34	6.3	81.9	81.30	5.2
XP	180°C/ 1h	276.14	146.60	6.5	82.5	77.38	5.3
XL	180°C/ 12h	317.09	147.51	6.5	86.1	81.10	5.3
XI	180°C/ 24h	324.53	155.43	6.5	87.4	87.10	5.3

The results of the structural analysis of the experimental samples concerning the metallographic aspects after the application of different heat treatments of Al-Mg rolled aluminium samples are shown in **Fig. 23**. It can be noticed that in the control sample there is a dendritic appearance of the sample (**Fig. 23a**), with small amounts of particles precipitated dendritically. By applying ageing, homogenisation of the matrix occurs, with the particles still in dendritic separation (**Fig. 23 b-g**).

Experimental results on grain size determination after statistical analysis of experimental samples are shown in Fig. 24.

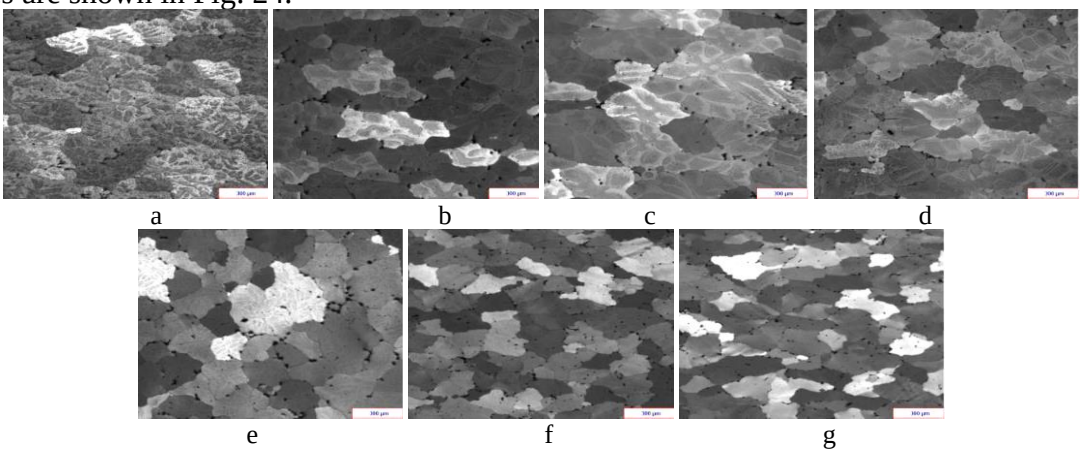

Fig. 23 Structural analysis of experimental rolled samples of aluminum alloy Al-Mg: (a) gauge sample (X), (b, c, d) ageing at 140°C; (e, f, g) ageing at 180°C; (b, e - 1h); (c, f -12h); (d, g- 24h).

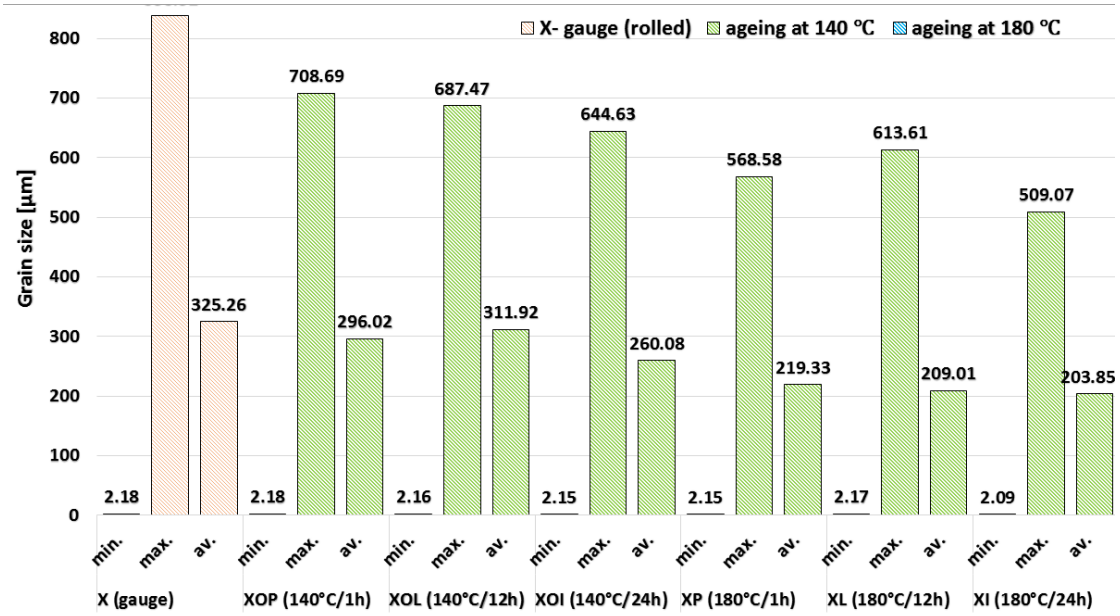

*Fig. 24 **G**rain size histogram of the experimental rolled Al-Mg alloy samples, in different structural state.*

Qualitative phase analysis using the X-ray diffraction method revealed the polycrystalline state of the studied samples, as shown in **Fig.25**. A careful analysis of the values of the elements in the elemental cell revealed that the application of thermal ageing treatments can lead to a change in this parameter compared to the control sample. An increase of the lattice parameter can be observed in the range 4.073 ÷ 4.079 [Å] when applying the ageing heat treatments at 140°C / 180°C, respectively at 24h durations, at 140°C ageing, the lattice parameter increases by 0.05%.While when increasing the holding durations at 24h, 180°C ageing there is an increase of the lattice parameter of 0.2%.

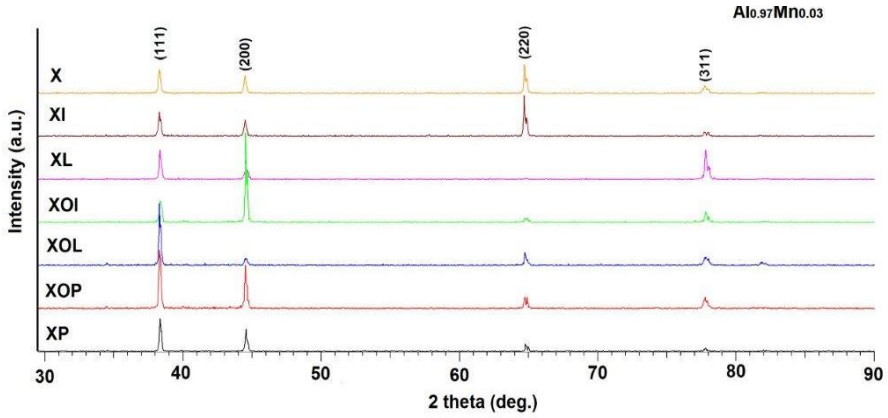

Fig. 25– X-ray diffractograms of rolled Al-Mg aluminum alloy samples in different structural states.

The determination of the cavitational erosion behaviour of the experimental specimens is shown in Fig. 26.

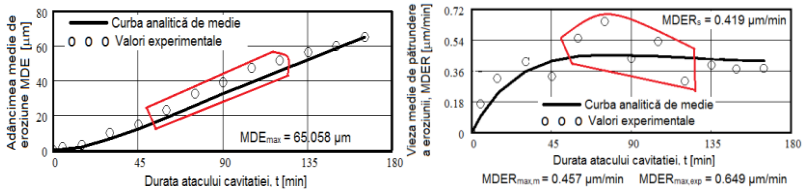

A = 0.4, B = 0.026

a b

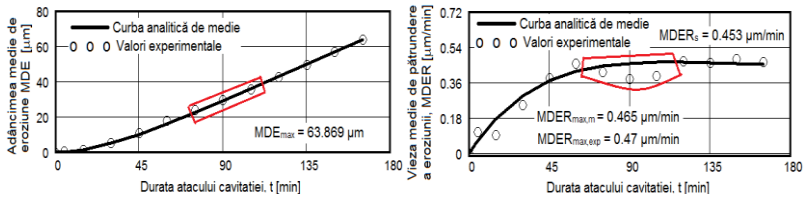

A = 0.41, B = 0.017

c d

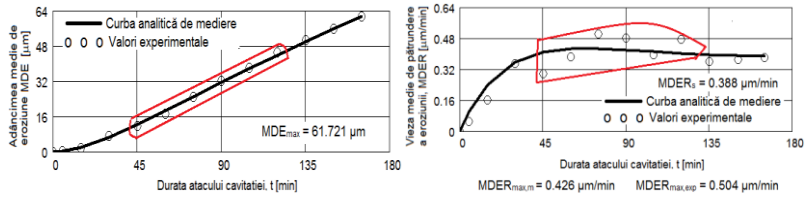

A = 0.377, B = 0.029

e f

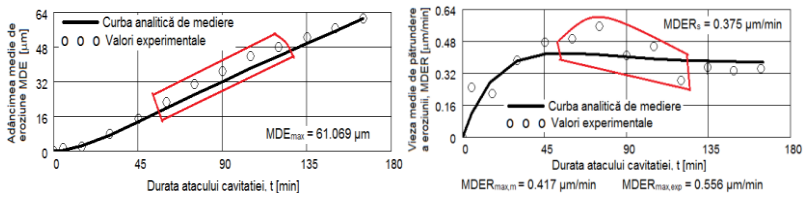

A = 0.371, B = 0.014

g h

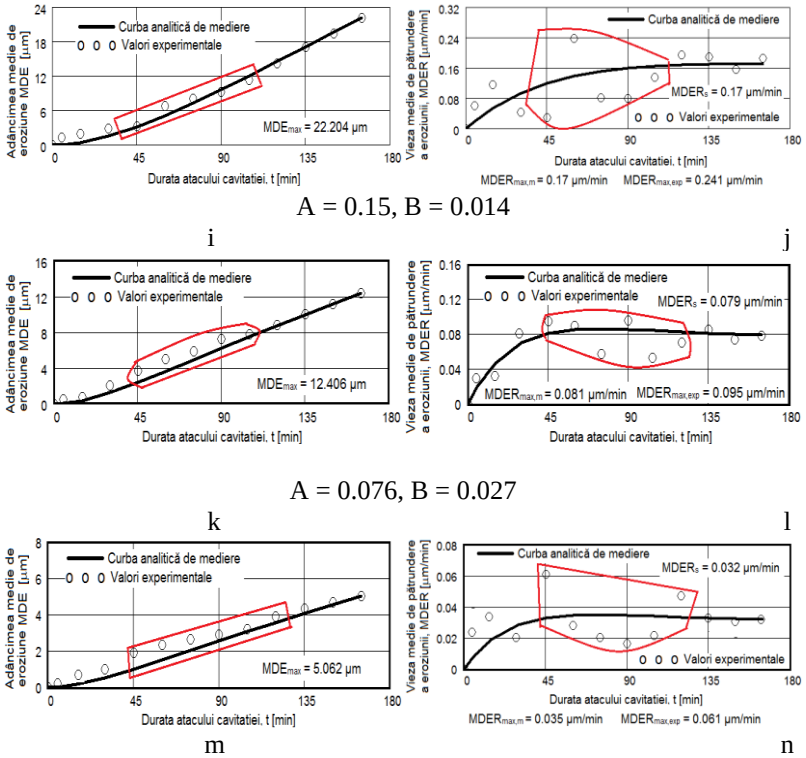

Fig. 26– Average erosion depth (a, c, e, f, g, i, k, m) and average erosion rate (b, d, f, h, i, l, n) vs cavitation exposure time of experimental samples of aluminum Al-Mg alloy: (a, b) - gauge sample; 296 (c, d, e, f, g, h) ageing at 140°C; (i, j, k, l, m, n) ageing at 180°C; Holding times: (c, d, i, j) - 1h; (e, f, k, 297 l) - 12 h; (g, h, m, n) - 24 h.

A careful analysis of these graphs, whose comparative results are illustrated in **Tab. 8** and **Tab.9**, show that the rolled Al-Mg alloy specimens show similar behaviour with the same erosion mechanisms, specific to the aluminium alloy class, much different from the erosion mechanisms found in other classes of solid state hardenable metallic materials. Cavity erosion of the surface is initiated as early as 15-30 minutes, but substantial, large losses occur, with the creation of deep caverns in depth, in the form of crocks, which increase greatly in geometrical dimensions in the range 60÷120 minutes. From minute 135 onwards, the caverns develop less, for the reasons mentioned (penetrating air dampening the impact pressure). The macrostructural aspects revealed by stereomicroscope capture the extension of cavitational attack in the frontal section. The control specimen has the most extensive surface affected by cavitational attack, while the specimens heat-treated at 180°C show the smallest surfaces affected by cavitational attack. Detailed cross-sectional analysis of the surfaces under cavitational stress (right images of **Fig. 27÷ Fig. 31**) allowed both profile visualization and determination of the maximum penetration depth of the cavitational attack. Note the difference between the measured maximum cavitational depth value trapped in the sectioning plane (found in the range 382 ÷ 175 µm, **Fig. 27 ÷ Fig.29**) and the cumulative maximum mean value calculated after 165 minutes (found in the range 65 ÷ 5 µm, **Fig. 27**), a difference of about 4 ÷ 35 times. It is reconfirmed that for the assessment of the strength and behaviour of a structure to cavitational attack stress it is recommended to use the surface average value MDEmax calculated at the end of the test and not the maximum value of a cavern, from an arbitrary area. However, the very large value of the cave trapped in the sectional plane raises a big question mark of the fineness and structure constitution of an aluminium alloy with or without preliminary heat treatment. This behaviour may give clues to the mechanics of the cavitational phenomenon between different structural classes of metallic materials. Where the surface hardening mechanism occurs in volume, following a solid state transformation, the differences are minimal. Where the surface hardening mechanism occurs only by solid solution hardening (as is the case with aluminium

alloys), then the differences are particularly high, due to the formation of deep local caverns around the hardening particles in a solid solution mass unaffected by cavitational attack. Scanning electron microscopic analysis of cavitationally eroded surfaces adds to the information on surface morphology as well as on the mechanism of cavitational crack propagation in this class of metallic materials. Thus, as shown in **Fig. 28**, in the case of a non-heat-treated specimen in the rolled state, on the macroscopic scale the surface appears almost uniformly eroded with numerous large-area, polygonal-shaped cavitations (**Fig. 28a**). On microscopic analysis (**Fig. 28b**) the surface of the cavitated bottom is cleaved, brittle, faceted and bounded by numerous secondary cracks. In the heat-treated samples by ageing the aspects of the cavitated surfaces are approximately similar, in contrast to the cavitations frequency as well as the microscopic appearance. Thus, for example, in an ageing heat-treated surface la140°C / 12h/air (**Fig. 29a**) at the macroscopic scale the surface shows a high frequency of cavitations, with rounded edges, of relatively small size (0.1-0.5mm). On microscopic analysis (**Fig. 29d**) the surface has a brittle, cleaved, faceted appearance with numerous intergranular secondary cracks.

A careful analysis of these graphs, whose comparative results are illustrated in **Tab. 5** and **Tab. 6**, show that the rolled Al-Mg alloy specimens show similar behaviour with the same erosion mechanisms, specific to the aluminium alloy class, much different from the erosion mechanisms found in other classes of solid-state hardenable metallic materials. The data in **Tab. 6** highlights the differences between the experimentally obtained maximum (MDERmax,exp) and maximum (MDERmax,m) and stabilization (MDERs) values, defined by the MDER(t) curves. The high values of these differences may create the impression that we have a structure with poor cavitational strength, typical of materials with large grain sizes, high numbers of structural defects (such as intermetallic compounds) and low values of mechanical properties, especially hardness. In this case we consider that these differences cannot be attributed to the strength of the structure, but rather to the damping effect of cavitational air and to the hardening of the layer under repetitive impacts of cavitational microjets. On the other hand, the high values of the velocities, whatever they are, are indicative of cavitational resistance and correspond to the appearance of the microscopic images in **Fig. 27- Fig. 29**. Therefore we judge that, according to the value of the velocities defined by the curves, the highest resistance is of the structure of sample XI (treated at 180 ^{0}C with duration of 24 hours) and the lowest of sample XOP (treated at 140 ^{0}C with duration of one hour). According to the range of values, we estimate that the samples (X, XOP, XOL and XOI) have cavitational strengths of the same order, clearly lower than XL and XI, with XP being of intermediate strength. Therefore the data in **Tab. 6** are expressions of the influence of structure on cavitational strength by the heat treatment regime parameters, through microstructural changes and mechanical property values. The data in **Tab. 7** give similar conclusions as those recorded in **Tab. 6** and from this we see that sample XI has the best resistance to cavitational erosion, with the average depth after 165 minutes of cavitating being significantly lower than the others. Compared to what was stated in **Tab. 5.4**, from **Tab. 5.5** it appears that the control sample (X) has the lowest resistance to cavitational attack. But it also follows that samples X, XOP, XOL and XOI have the structures with the lowest resistance to cavitational stresses. Both the data in Tab. 6 and those in **Tab. 7**, show that at 180 ^{0}C, irrespective of the holding time, the structures obtained have higher strengths than those obtained by ageing treatment at 140 ^{0}C, in the order of (2...13) times.

Tab. 8- Parameters of erosion-cavitation process of the rolled Al-Mg aluminum samples.

Sample	$MDER_{\max m}$	$MDER_{\max exp}$	$MDER_s$	Δ $\lvert MDER_{\max m} - MDER_{\max exp} \rvert$		Δ $\lvert MDER_{\max m} - MDER_{\max s} \rvert$	
				$\mu m/min$	%	$\mu m/min$	%
X	0.457	0.649	0.419	0.192	45.82	0.038	9.07

XOP	0.465	0.470	0.453	0.005	1.10	0.012	2.65
XOL	0.426	0.504	0.388	0.078	20.10	0.038	9.79
XOI	0.417	0.556	0.375	0.139	37.07	0.042	11.20
XP	0.170	0.241	0.170	0.071	41.76	0	-
XL	0.081	0.095	0.079	0.014	17.72	0.002	2.53
XI	0.035	0.061	0.032	0.026	81.25	0.003	9.38

Tab. 9 – The maximum penetration depth of the cavitation attack of the rolled Al-Mg aluminum alloy specimens, in different structural states.

Sample	**Maximum penetration depth of the cavitation attack**		
	$MDER_{max}$ (μm)	$\delta_{measured}$ (μm)	$MDER_{max}$ (μm)
X	65.058	382	6
XOP	63.869	297	5
XOL	61.721	279	5
XOI	61.069	223	4
XP	22.204	218	10
XL	12.406	205	17
XI	5.062	175	35

Macro and microstructural analysis of Al-Mg alloy specimens, rolled state, stressed by cavitational erosion is shown in **Fig. 27-Fig.29**.

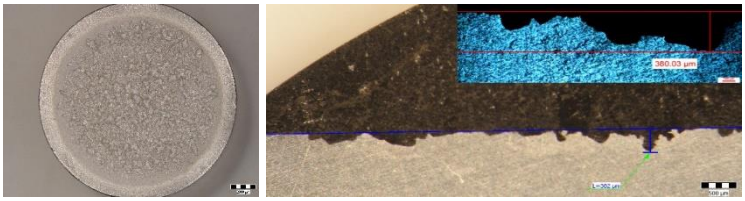

a) *b)*

Fig.27 - The appearance of surfaces subjected to cavitational erosion from rolled alloy Al-Mg, H111 (gauge sample) (piercer X):

a- stereomacrostructural image in section parallel to the eroded surface,
b- cross-section images (background – stereomicroscope image, upper left detail – optical micro scope image).

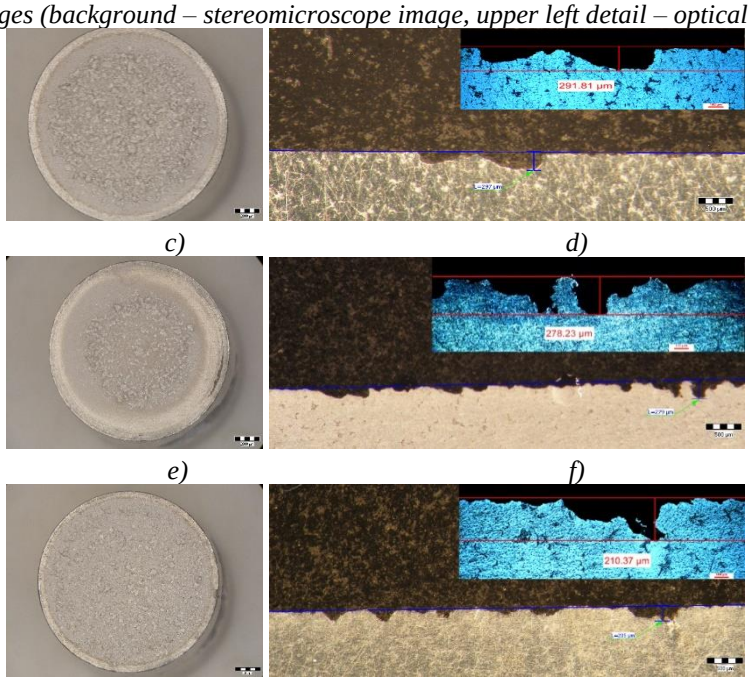

c) *d)*

e) *f)*

g) *h)*

Fig. 28 The appearance of the surfaces subjected to cavitational erosion from alloy Al-Mg, rolled state H111 followed by artificial ageing at 140°C and different holding times: (a, c, e) – stereo macro structural images in parallel section with the eroded surface, (b, d, f) - in cross section (background – stereomicroscope image, upper left detail – optical microscope image); (a, b) - 1h (piercer XOP); (c, d) – 12h (piercer XOL); (e, f) - 24 h (piercer XOI).

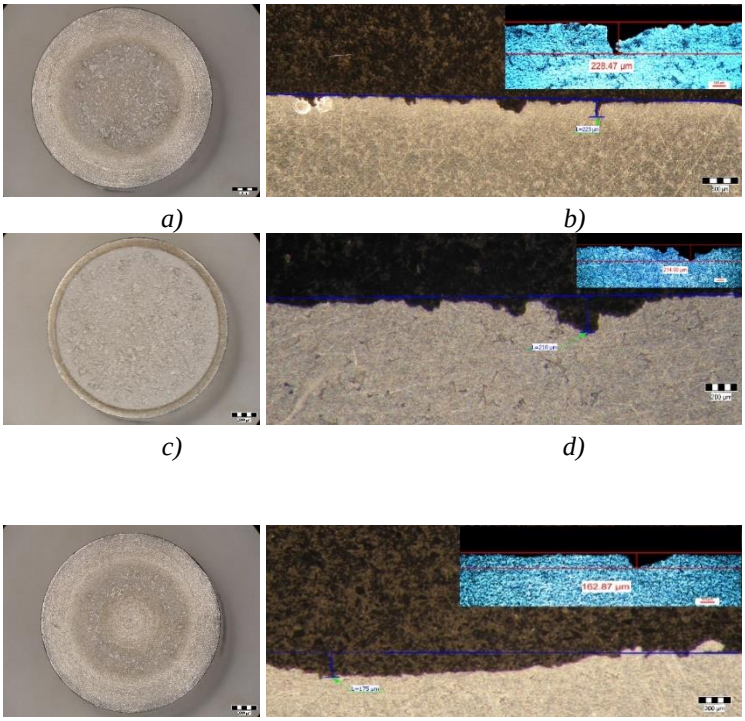

a) *b)*

c) *d)*

e) *f)*

Fig. 29 The appearance of the surfaces subjected to cavitational erosion from rolled alloy Al-Mg, state H111 followed by artificial ageing at 180°C C and different holding times: (a, c, e) – stereo macro- structural images in parallel section with the eroded surface, (b, d, f) - in cross section (background – stereomicroscope image, upper left detail – optical microscope image); (a, b) - 1h (piercer XP); (c, d) – 12h (piercer XL); (e, f) - 24 h (piercer XI).

Scanning electron microscope analysis of the cavitational eroded surfaces, shown in **Fig. 30**, completes the information on the morphology of the surfaces as well as on the mechanism of cavitational crack propagation in this class of metallic materials. Thus, as noted in **Fig. 30**, in the case of a non-heat-treated sample in the rolled state, the macroscopic surface appears almost uniformly eroded with numerous large-area, polygonal-shaped cavities (**Fig. 30a**). On microscopic analysis the surface of the cavitated bottom is cleavage-like, brittle, faceted and bounded by numerous secondary cracks. In the heat-treated samples by ageing the aspects of the cavitated surfaces are approximately similar, with a difference in the frequency of cavitations as well as in the microscopic appearance. Thus, for example in a 140^0C / 12h/air ageing heat treated surface (**Fig. 30b**) at the macroscopic scale the surface shows a high frequency of cavitations, with rounded edges, of relatively small size (0.1-0.5mm). On microscopic analysis the surface has a brittle, cleaved, faceted appearance with numerous intergranular secondary cracks. SEM analysis confirms a brittle behaviour of the Al-Mg aluminium alloy after cavitational erosion, the cavitations produced being generated by the secondary particles of the alloy, around which the structural integrity is destroyed, and there is no volume hardening of the material by the formation of a hard phase, with high mechanical properties (such as martensite), but only a hardening of the solid solution by precipitation of secondary phases (as in the case of the aluminium alloy Al-Mg (with hardening

phase Mg5Al8), following the interaction of the jet with the surface, dislocation of the particles occurs, leaving an eroded surface with numerous intergranular secondary cracks.

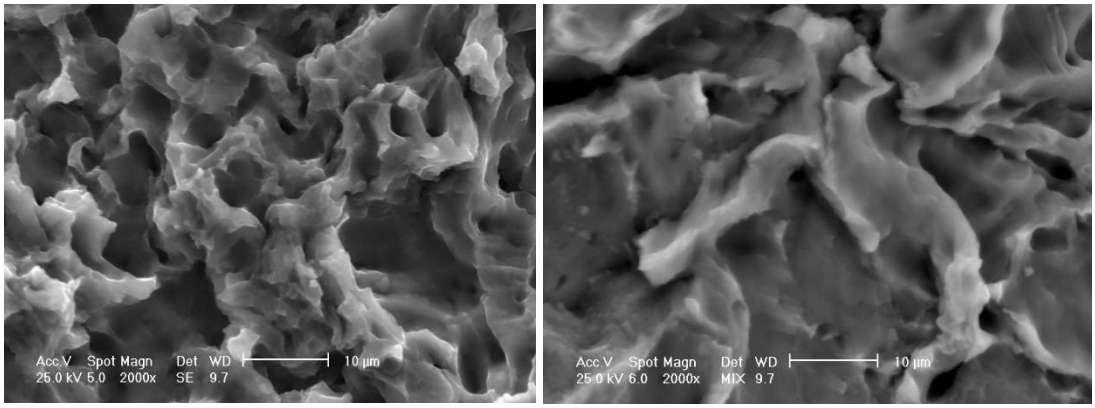

a b

Fig. 30- Scanning electron icroscope (SEM) analysis of eroded surfaces of Al-Mg alloy samples in H111 rolled state (a) and artificial softening at 140°C /12h (b)

Comparative analysis of the mechanical behaviour and cavitational erosion behaviour of Al-Mg aluminium alloy samples subjected to artificial ageing treatments at 140°C 1h, 12h, 24h and artificial ageing at 180°C /1h, 12h, 24h, allows the following interesting observations to be made from the experiments carried out in this thesis. The results are referred to the control sample.

Chapter 6 is entitled *Conclusions of the research undertaken in this paper. Original contributions, directions and perspectives of future experimental research*

6.1 Conclusions

- ✓ In the framework of the doctoral thesis, mechanical and structural analyses were carried out, optical microscope analyses, X-ray diffraction analyses, sterio-macro-structural analysis, SEM fractrographic analysis, determination of MDE(t) MDER(t) MDER and analyses to determine the hardness and microhardness values, determination of the grain size which allow us to formulate the following conclusions for the Al-Mg alloy in the cast state:
- ✓ After solution quenching at 350 °C /100 min + artificial ageing at 180°C the lowest cavitations penetration depths are obtained both with respect to the control sample, cast state, with 60μm and with respect to the samples subjected to solution quenching at 450 °C /100 min + artificial ageing (either at 140°C where the range of maximum penetration depths is 38-52μm, or at 180°C, where the maximum penetration depth is about 29μm).
- ✓ It can also be noted the correlation between the highest values of the mechanical characteristics obtained after application of solution quenching at 350 °C /100 min + artificial ageing at 180°C (1h, 12h, 24h) and the cavitational erosion behaviour, which is the most favourable for these heat treatments applied to Al-Mg aluminium alloy tuned products.
- ✓ By applying homogenisation heat treatments, either at 350°C or 450°C, followed by artificial ageing (140°C or 180°C), the mechanical and structural characteristics of Al-Mg alloy castings can be modified.
- ✓ Tensile strength and yield strength values are similarly modified. Thus, the highest values of these characteristics are recorded after homogenisation at 350°C + artificial ageing at 180°C / 24h (mechanical strength values are doubled and yield strength values are tripled compared to the control sample), cast condition.

- ✓ Elongation values are intermediate for homogenization at 350°C compared to homogenization at 450°C, regardless of aging time.
- ✓ Resilience values after heat treatment of homogenisation at 350°C + ageing at 180°C do not fall below 25J/cm2, regardless of ageing duration. Other heat treatments can lead to drastic decreases in resilience below 25J/cm^2 (such as after homogenisation heat treatment at 450°C + 140°C /12h, or 450°C + 140°C / 24h).
- ✓ Hardness values decrease slightly after homogenisation at 350°C + 180°C (only 1-4%), compared to homogenisation at 450°C + 140°C, where hardness decreases up to 10% compared to the control sample.
- ✓ The lowest mean grain size values are for homogenisations at 350°C + 180°C, mean grain sizes for homogenisations at 450°C + 140°C and the highest grain sizes at 450°C + 180°C.
- ✓ By applying heat treatments to Al-Mg alloy castings, either solution quenching at 350 °C /100 min + artificial ageing at 180°C (1h, 12h, 24h) or solution quenching at 450 °C /100 min + artificial ageing at 140°C (1h, 12h, 24h) or solution quenching at 450 °C /100 min + artificial ageing at 180°C (1h, 12h, 24h) can increase resistance to cavitational corrosion in terms of decreasing depths and erosion penetration rates.
- ✓ In the same combination of heat treatments, increasing the artificial ageing retention time results in decreasing the maximum cavitational penetration depths.

After solution quenching at 350°C /100 min + 180°C (Fig. 4.19 c, d, e, f, g, h) the maximum depth of cavitations MDEmax, decreases from 17,928 μm (at 1h holding), to 15,128μm (at 12h holding), reaching 14,572 μm (at 24h holding). After solution quenching at 450°C /100 min + 140°C (Fig. 4.19 i, j, k, l, m, n) the maximum depth of cavitations MDEmax decreases from 52,115μm (at 1h holding), to 43,017μm (at 12h holding), reaching 38,31 μm (at 24h holding). After solution quenching at 450°C /100 min + 180°C (Fig. 4.19 o, p, r, s, t, u) the maximum depth of cavitations MDEmax decreases from 29,572μm (at 1h holding) to 29,471μm (at 12h holding) to 28,589 μm (at 24h holding).

The best combination of heat treatments applied to Al-Mg aluminium castings is homogenisation at 350°C followed by artificial ageing at 180°C, at which the best mechanical characteristics are obtained, a resilience of 25 J/cm^2, a scratch size of 140-180μm and maximum MDEm erosion depth around 14-17 μm.

Heat treatment applied to Al-Mg series aluminium alloys, cast state, leads to stabilization of the phase composition, but also of the alloy structure such as: size, quantity, shape, distribution of secondary phase separations in grain volume and on their separation boundary, grain size itself of α-solid solution as well as of crystallized primary phases.

- ✓ Usually, at higher temperatures, (diffusion is more active), the separation process is more advantageous on the grain boundary, and at lower temperatures solid α-solution appears to a higher degree inside the grains .
- ✓ And at the same time the following conclusions can be formulated for the Al-Mg alloy rolled state.
- ✓ The application of artificial ageing heat treatments (140°C or 180°C) can lead to changes in the mechanical and structural characteristics of Al-Mg aluminium alloy laminates in different proportions.
- ✓ Fracture strength values show a smaller increase for artificial ageing at 140°C/1, 12, 24h (maximum 9%) and a larger increase for artificial ageing at 180°C/1, 12, 24h (up to 35%).
- ✓ The values of the yield strength increase up to a maximum of 14% when applying artificial ageing heat treatments at 140°C/1, 12, 24h, while after applying artificial ageing heat treatments at 180°C/1, 12, 24h the yield strength can reach up to 23%.
- ✓ The elongation values show that they are very little influenced by the application of the ageing treatment, being in the tight range of 6.3 ÷ 6.5%.

- ✓ The resilience values after application of the ageing treatment at 140°C / 180°C do not change significantly compared to the control sample, the values being in the range 5.2 ÷ 5.3 J/ cm^2.
- ✓ The hardness values decrease slightly or are maintained after the application of the ageing treatment at 140°C / 180°C compared to the control sample, except for the hardness value after ageing at 180°C/24h with an increase of about 2%.
- ✓ By applying artificial ageing heat treatments at 140°C (1h, 12h, 24h) and 180°C (1h, 12h, 24h) to Al-Mg alloy rolled products, the resistance to cavitational corrosion can be increased, in the sense of decreasing the penetration depths and the erosion penetration rate. Thus, after ageing at 140°C the maximum cavity penetration depth MDEmax is 63.869μm (at holding 1h), at 61.721μm (at holding 12h), and at 61.069μm (at holding 24h). After aging at 180°C the maximum penetration depth of the MDEmax cavity is 22.204μm (at 1h hold), at 12.406μm (at 12h hold), and at 5.062μm (at 24h hold)
- ✓ In all samples, regardless of whether it is blank or thermally rolled, after 105 (120) minutes of cavitation and until the end of the test, the erosion is carried out at an approximately constant rate, which leads to a linear variation of the MDE(t) curve and the tendency to maintaining the maximum value, or slightly decreasing (asymptotically) towards the stabilization value of the MDER(t) curve. The explanation is related to the air penetrated into the voids left by the expulsion of the material, which attenuates the impact force and as a consequence the expansion of the cracks, the breaking of the links between the grains and their expulsion.
- ✓ Regardless of the holding time (one hour, 12 hours or 24 hours) at the temperature of 140°C of the artificial aging treatment, there is a time interval, between 45-120 minutes, in which the erosion manifests itself profoundly by increasing number and geometric dimensions of pinches and caverns. The difference between the sizes of this interval depends on the duration of holding at the temperature of 140°C, which determined differences between the values of the mechanical properties and the type of microstructure.
- ✓ The differences between the maximum values of the maximum depths measured in the axial plane of sectioning and the approximation curves, after the completion of the test (165 minutes), are of the order of 4-6 times. This observation reconfirms that the maximum depth measured in an axial section (dependent on the place of sectioning) is not an indicator that serves to compare the strength of the surface after the applied treatment.
- ✓ The attack times at which the highest values are recorded for the speed determined experimentally and that defined by the MDER(t) averaging curve are different. The explanation is related to the mass of grains (intermetallic compounds) expelled in certain phases of cavitation stress.
- ✓ The shapes of the caverns, from pinched to united caverns, with different depths, are mainly determined by the shape of the microstructure resulting from the heat treatment regime applied.
- ✓ From the point of view of the influence of the holding time at the artificial aging temperature at 140°C, the structure that has the highest resistance to cavitation erosion is obtained for the duration of 24 hours and with lower resistances, of close order, for the durations of 1h and 12h.
- ✓ From the point of view of the influence of the holding time at the artificial aging temperature at 180°C, the structure with the highest resistance to cavitation erosion is obtained for the holding time of 24 hours, and the structure with the lowest cavitation resistance is the one to maintain for one hour.
- ✓ Considering a quantitative parameter obtained during the stereomacrostructural analysis, the value of the ratio between the diameter of the area most affected by cavitational erosion

and the initial diameter, it is observed that the value of this parameter is very high in the control sample, about 85%, it is lower after artificial aging at 140 °C, of about 80%, reaching much lower values after applying an artificial aging at 180°C (up to 56%).

- ✓ The best results regarding thermal aging treatments applied to Al-Mg type aluminum laminated products are obtained after artificial aging at 180°C/24h maintenance, with the best mechanical characteristics, breaking strength 324.53 [MPa], yield strength of 155.43[MPa], hardness of 87.4 [[MPa]], an average grain size of 203.85 μm, a maximum depth of cavitational erosion MDEmax of 5 μm and the smallest ratio between the diameter of the most affected area and the initial diameter of the specimen , of about 52%.

6.2 Original contributions

The research topic addressed in the doctoral thesis presents an original character, the results being obtained following a complex research program. The personal contributions made in the field of improving the surface subjected to erosion by cavitational attack of Al-Mg type aluminum alloy, in different structural states, are presented in the following:

- ✓ Investigation of a large number of Al-Mg type alloy samples, in different structural stages. For the cast state, solution heat treatments were carried out at different temperatures with well-established holding times, followed by artificial aging at different temperatures and different holding times. For the laminated state, artificial aging thermal treatments were performed at different temperatures with different holding times, which were correlated with the evaluation of resistance to cavitational erosion;
- ✓ Completing a database for Al-Mg type aluminum alloy to support the specialized literature and the various fields of industry where the cavitation phenomenon can intervene with catastrophic effects
- ✓ Complete investigation of a large number of samples to highlight structural aspects, with the help of modern characterization techniques (X-ray diffraction, stereomacroscopy, optical microscopy and scanning electron microscopy).
- ✓ Demonstration by means of various modern structural investigation methods of the cavitational behavior of Al-Mg type aluminum alloy. Through the investigations carried out at the macro and microstructural level, correlations between the phasic constitution and the cavitational behavior in laboratory conditions could be achieved.
- ✓ Complex characterization from the mechanical point of view by determining the main mechanical characteristics of the Al-Mg type aluminum alloy (determining the microhardness values, determining the mechanical tensile strength and yield limits).
- ✓ Macrostructural analyzes were taken into consideration (by quantitatively determining the average diameter of the surface affected by cavitation, determining the surface affected by the cavity, as well as determining the maximum penetration depth of cavitation), which allowed a tie-breaker regarding the resistance state of the materials to cavitation. Thus, it can be proposed as a quick measure of material selection in terms of cavitation resistance with the help of a relatively simple analysis, namely stereomacrostructural analysis, without further investigations at very high magnification powers.
- ✓ The use of simple methods of quantitative and qualitative assessment, in cross-section, of the main cavitational structural aspects. The evaluation methods took into account the

macroscopic analysis and the microscopic analysis in cross-section, which allowed the dimensional determination of the caverns produced by cavitation in the different areas of the samples.

6.3 Directions and perspectives of future experimental research

- ✓ Following the research and analysis of the Al-Mg alloy samples in the cast state and the rolled state within the thesis, some new or current aspects were identified that can be taken into account or improved.
- ✓ Al-Mg aluminum alloys in cast state and rolled state are still sources of future, experimental research, for increasing performance in their exploration and use in the field in which they are subject to cavitational attack, and finding / establishing a thermal treatment of homogenization / artificial ageing, to meet the current exploitation requirements.
- ✓ It is also possible to use the specific techniques of stereomicroscopy in the assessment and analysis of the state of the surfaces, both cast and deformed, or of the surfaces that are subjected to cavitational attack.

LIST OF PUBLISHED WORKS

Published articles, ISI rated, in international journals1. **ISTRATE** D.; Sbârcea B.-G.;Demian A.M.; Buzatu A.D.Salcian L.; Bordeasu, I.; Micu L.M.; Ghera C.; Florea B.; Ghiban B. - Correlation between Mechanical Properties—Structural Characteristics and Cavitation Resistance of Cast Aluminum Alloy Type Al-Mg. Crystals 2022, 12, 1538. https://doi.org/10.3390/ cryst12111538

2. Ilare BORDEASU, Brandusa GHIBAN, Vasile NAGY, Vlad PARAIANU, Cristian GHERA, Dionisie **ISTRATE**, Alin Mihai DEMIAN, Petrisor - Ovidiu ODAGIU - Cavitational erosion resistance considerations for alloy 6082 state t651 - U.P.B. Sci. Bull., Series B, Vol. 85, Iss. 1, 2023, ISSN 1454-2331

3. Dionisie **ISTRATE**, Ilare Bordeasu, Brândusa Ghiban, Bogdan Istrate, Beatrice-Gabriela Sbarcea, Cristian Ghera, Alexandru Nicolae Luca, Petrisor Ovidiu Odagiu, Bogdan Florea, Dinu Gubencu. - Correlation between Mechanical Properties—Structural Characteristics and Cavitation Resistance of Rolled Aluminum Alloy Type Al-Mg. Metals 2023, 13, 1067. https://doi.org/10.3390/met13061067

Articles published, BDI rated, in specialized journals1. Dionisie **ISTRATE**, Cristian GHERA, Laura SĂLCIANU, Ilare BORDEAȘU, Brândușa GHIBAN, Dumitru Viorel BĂZĂVAN, Lavinia Mădălina MICU, Daniel-Cătălin STROIȚĂ, Daniel OSTOIA-Heat Treatment Influence of Alloy Al-Mg on Cavitational Erosion Resistance, Magazine of Hydraulics, Pneumatics, Tribology, Ecology, Sensorics, Mechatronics, ISSN 1453 – 7303, HIDRAULICA" (No. 3/2021) Pages 15-25

2. Ilare BORDEAȘU, Cristian GHERA, Dionisie **ISTRATE** , Laura SĂLCIANU, Brandușa GHIBAN, Dumitru Viorel BĂZĂVAN, Lavinia Mădălina MICU , Daniel-Cătălin STROIȚĂ , Alexandra SUTA, Ileana TOMOIAGĂ, Alexandru Nicolae LUCA- Resistance and Behavior to Cavitation Erosion of Semi-Finished Aluminum Alloy Al-Mg, Magazine of Hydraulics, Pneumatics, Tribology, Ecology, Sensorics, Mechatronics, ISSN 1453 – 7303, HIDRAULICA" (No. 4/2021) Pages 17-24

3.Alexandru Nicolae LUCA, Ilare BORDEAȘU, Brândușa GHIBAN, Cristian GHERA, Dionisie **ISTRATE**, Cătălin STROIȚĂ- MODIFICATION OF THE CAVITATION RESISTANCE BY HARDENING HEAT TREATMENT AT 450 °C FOLLOWED BY

ARTIFICIAL AGING AT 180 °C OF THE ALUMINUM ALLOY Al-Mg COMPARED TO THE STATE OF CAST SEMI-FINISHED PRODUCT, Magazine of Hydraulics, Pneumatics, Tribology, Ecology, Sensorics, Mechatronics, ISSN 1453 – 7303, HIDRAULICA" (No. 1/2022) Pages 39-45

4. Dionisie **ISTRATE**, Claudia Lazar (Natra), Ovidiu Petrisor Odagiu, Alin Mihai Demian, Andreea Daniela Buzatu, Brandusa Ghiban - Influence of homogenization and aging parameters applied to mechanical and structural characteristics of alloy Al-Mg, ACME-02-01: Materials and Surface Engineering, June 9th, 2022, ACME , Iași, code, 2-015

5. Claudia Lazar (Natra), Dionisie **ISTRATE**, Ovidiu Petrisor Odagiu, Alin Mihai Demian, Andreea Daniela Buzatu, Brandusa Ghiban- Evaluation of mechanical characteristics of 3003 aluminum alloy plated sheets, ACME-02-01: Materials and Surface Engineering, June 9th, 2022, ACME, Iași, code, 2-016

Articles presented at national and international conferences

1. L M Micu, I Bordeasu, **ISTRATE** Dionisie, B Ghiban and D Gubencu - Influence of aging heat treatment at 180 0C on cavitation erosion for aluminum alloy type Al-Mg in cold rolled state - INTERNATIONAL CONFERENCE ON APPLIED SCIENCES ICAS2022, Banja Luka, Bosnia and Herzegovina, May 25-28, 2022

2.Dionisie **ISTRATE**, Alin Mihai DEMIAN, Andreea Daniela BUZATU, Petrisor- Ovidiu ODAGIU, Brândușa GHIBAN -The influence of heat treatments on the mechanical and structural characteristics of plastically deformed type Al-Mg aluminum alloys - 9th International Conference on Materials Science and Technologies – RoMAT 2022 November 24-25, 2022, Bucharest, Romania

3. A. D. Buzatu, D. **ISTRATE**, A. M. Demian, P.- O. Odagiu, B. Ghiban - Heat treatments influence on the mechanical behavior and structural characteristics of aluminum alloys type 2017 -- 9th International Conference on Materials Science and Technologies – RoMAT 2022 November 24-25, 2022, Bucharest, Romania

4.P.- O. Odagiu, D. **ISTRATE**, A. M. Demian, A. D. Buzatu, B. Ghiban-The influence of thermal treatments on the mechanical and structural characteristics of aluminum alloys type 6082-- 9th International Conference on Materials Science and Technologies – RoMAT 2022 November 24-25, 2022, Bucharest, Romania**.**

5. A. M. Demian, A. D. Buzatu, P.- O. Odagiu, D. **ISTRATE**, B. Ghiban - Heat treatments influence on the mechanical and structural characteristics of 7075 aluminum type alloys-- 9th International Conference on Materials Science and Technologies –RoMAT 2022 November 24-25, 2022, Bucharest, Romania

Selective Bibliography

1. Shayganpour A., "'Evaluation of signifiant factors in aluminum lost foam casting using doe approach," Universiti Teknologi Malaysia, December 2010.
2. Stoian F., Piaţa internaţională a aluminiului în 2014 (International Aluminium Market in 2014), Conjunctura Economiei Mondiale, 2015.
3. IOAN FARA –Aluminiul de la materia primă la produse finite-Editura tehnică-2000.
4. http://www.google.ro/search?q=produse+din+aluminiu&bav=on.2,
5. Lăzărescu I., - Aluminiul, Editura Tehnică, Bucureşti, 1978.
6. Moldovan P. ș.a. – Tratat de ştiinţa şi ingineria materialelor metalice, vol.2, Editura AGIR, Bucureşti, 2007.
7. Sporea I., Bordeaşu I., Mandek F., Aliaje de aluminiu refractare turnate în pistoane de motoare termice Editura Politehnica Timișoara 2008 ISBN 978-973-625-627-1, România.
8. Gâdea S., Protopopescu, M, – Aliaje neferoase, Editura Tehnică, Bucureşti, 1965.
9. Apelian D., "'Aluminium Cast Alloys: Enabling tools for improved performance," NADCA, 2009.
10. Pickin C, G., Young K., - Evaluation of cold metal transfer (CMT) process for welding aluminium alloy, Science and Technology of Welding and Joining vol. 11, nr. 4. 2006.

11. KIM S J, JANG S K, KIM J I, Investigation on optimum corrosion protection potential of Al alloy in marine environment [J], Materials Science, 2008, 26(3): 779_786
12. SON I. J, NAKANO H, OUE S, KOBAYASHI S, FUKUSHIMA H, HORITA Z, Effect of annealing on the pitting corrosion resistance of anodized aluminum_magnesium alloy processed by equal channel angular pressing [J], Corrosion Science and Technology, 2007, 6(6): 275_281.
13. SAKAIRI M, SHIMOYAMA Y., NAGASAWA D., Electrochemical random signal analysis during localized corrosion of anodized 1100 aluminum alloy in chloride environments [J], Corrosion Science and Technology, 2008, 7(3): 168_172.
14. HAN M. S., LEE S.. J, JANG S K, KIM S J, Electrochemical and cavitation characteristics of Al thermal spray coating with F_Si sealing [J], Corrosion Science and Technology, 2010, 9(6): 317_324.
15. KIM S. J., LEE S. J., Investigation on electrochemical and cavitation characteristics of rudder materials for ship in sea water [J], Corrosion Science and Technology, 2011, 10(3): 101_107.
16. L. Kramer, M. Phillippi, W.T. Tack, C. Wong, Locally reversing sensitization in Al-Mg aluminum plate, J, Mater, Eng, Perform, 21 (6) (2012) 1025–1029.
17. M.-S., Han, S. Ko, S.-H. Kim, S.-K. Jang, S.-J. Kim, Optimization of corrosion protection potential for stress corrosion cracking and hydrogen embrittlement of Al-Mg-H112 alloy in seawater, Met, Mater, Int, 14 (2) (2008) 203–211.
18. Escaler X., Farhat M., Avellan F., Egusqiza E., Cavitation Erosion Test on a 2D Hydrofoil Using Surface Mounted Obstacles, Wear, 2003, Vol.254: p. 441.
19. Vyas B, and C.M. Preece, Cavitation erosion of face centred cubic metals, Metallurgical and Materials Transactions A. 1977, Vol.8: p. 915-923.
20. Fedokin I. and O. Yachno, Some problems of development of cavitation technologies for industrial applications, in CAV2001,Cavitation Technology, 2001, Proceedings of the Fourth International Symposium on Cavitation: California Institute of Technology, Pasadena, USA .
21. Brennen C.E., Cavitation and Bubble Dynamics, 1995, New York: Oxford University Press.
22. R.P. Jewett, J.A.H., in: E.A. Loria (Ed.), Superalloys 718, 625, 706 and Various Derivatives, The Minerals, Metals and Materials Society, Warrendale, PA, 1991: p.749-760.
23. V. GarcíaNavas, I.A., O.Gonzalo, J.Leunda., Int.J.Mach,ToolsManuf., 2013, 74: p. 19-28.
24. Schwartz A.J., M, Kumar, and B.F, Adams, D. P., Electron Backscaterring microscopy in Materials Science, Springer, New York, 2009, 107: p.414-421.
25. J.H., Chen, W,W., Mater. Sci. Eng. A. 2008, 489: p. 451-456.
26. S. Hattori, T.I., Wear, 2011, 271: p. 1103-1108.
27. B. Karunamurthy, M.H., C.Vieillard. G.E.Morales-Espejel, Z.Khan, . Ceram, Int., 2010, 36: p. 1373-1381.
28. J.J. Lu, K.H.Z.G., J.Schneider, Wear, 2008, 265: p. 1680-1686.
29. J. Stella, T.P., M.Pohl, Wear, 2013, 300: p. 163-168.
30. M.C. Park, G.S.S., J.Y.Yun.J.H.Heo.D.Kim.S.J.Kim., Wear, 2014, 310: p. 27-32
31. G. Gottardi, M. Tocci, L. Montesano, A. Pola, Cavitation erosion behaviour of an innovative aluminium alloy for hybrid aluminium forging, Wear 394 (2018) 1–10.
32. S. Zhang, S. Wang, C.L. Wu, C.H. Zhang, M. Guan, J.Z. Tan, Cavitation erosion and rosion-corrosion resistance of austenitic stainless steel by plasma transferred arc welding, Eng, Fail, Annal, 76 (2017) 115–124.
33. W. Liu, The microscopic features of cavitation erosion and the solution in the plastic injection moulding machines, Eng. Fail, Annal, 36 (2014) 253–261.
34. D.G. Li, D.R. Chen P. Liang, Enhancement of cavitation erosion resistance of 316 Lstainless steel by adding molybdenum, Ultrason, Sonochem, 35 (2017) 375–381.
35. M. Hajian, A. Abdollah-zadeh, S.S. Rezaei-Nejad, H. Assadi, S.M.M. Hadavi, K. Chung, M., Shokouhimehr, Improvement in cavitation erosion resistance of AISI316L stainless steel by friction stir processing, Appl. Surf. Sci. 308 (2014) 184–192.
36. S. Hanke, A. Fischer, M. Beyer, J. Santos, Cavitation erosion of NiAl-bronze layers generated by friction surfacing, Wear 273 (2011) 32–37.
37. A. Pola, L. Montesano, M. Tocci, G.L. Vecchia, Influence of ultrasound treatment on cavitation erosion resistance of AlSi7 alloy, Mater 10 (2017) 256.
38. A. Jayaprakash, J.K. Choi, G.L. Chahine, F. Martin, M. Donnelly, J.P. Franc, A. Karimi, Scaling study of cavitation pitting from cavitating jets and ultrasonichorns, Wear 296 (2012) 619–629.
39. H.C. Man, C.T. Kwok, T.M. Yue, Cavitation erosion and corrosion behaviour of laser surface alloyed MMC of SiC and Si3N4 on Al alloy AA6061, Surf. Coat, Technol, 132(2000) 11–20.
40. Bordeaşu I., Eroziunea cavitaţională asupra materialelor utilizate în construcţia maşinilor hidraulice şi elicelor navale, Efecte de scară., Timişoara, 1997.
41. Bordeasu I.: Monograph of the Cavitation Erosion Research Laboratory of the Polytechnic University of Timisoara (1960-2020), Editura POLITEHNICA, ISBN 978-606-35-0371-9, Timisoara 2020.

42. Garcia R., Hammitt F. G., Nystrom R.E., Corelation of cavitation damage with other material and fluid properties, Erosion by Cavitation or Impingement, ASTM, STP 408 Atlantic City, 1966.
43. Steller K., Reymann Z., Krzysztoowicz T: Evaluation of the resistance of materials to the cavitational erosion, Procedings of the fifth Conference on Fluid Machinery, Vol 2, Akad Kiado, Budapest, 1975.
44. Leng Y., Materials characterization, Introduction to microscopic and spectroscopic methods, 2008, Singapore: John Wiley & Sons Pte Ltd.
45. Geru N., and M. Bane, Analiza structurii materialelor metalice, 1991, București: Editura Tehnică.
46. Bojin D., F. Miculescu and M. Miculescu, Microscopie electronică de baleiaj și aplicații, 2005, București: Editura Agir.
47. Michette A. and S. Pfauntsch, X-Ray: The first hundred years, 1996, New York: John Wiley&Sons Inc.
48. He B.B., Two-dimensional X-ray diffraction, 2009, SUA: John Wiley&Sons Inc.
49. Călțun O.F., Ferite de cobalt magnetostive, 2008, Iasi: Editura Universitatii "Alexandru Ioan Cuza".
50. Reed, R.C., The Superalloys: Fundamentals and Applications, Cambridge: Cambridge University Press, 2008.
51. Saarimäki, J., The Mechanical Properties of Lattice Truss Structures with Load- Bearing Shells Made of Selectively Laser Melted Hastelloy XTM, KTH, 2011.
52. "Solid Solution Hardening - an overview, www.sciencedirect.com, 2018.
53. Standard test method for cavitation erosion using vibratory apparatus, 2010 ASTM G32-2010,ASTM International., 2010.
54. Bordeaşu I., P.M.O., Patrascoiu C-tin, Bălăsoiu V., „An Analytical Model for the Cavitation Erosion Characteristic Curves", Transaction of Mechanics, Timisoara, 2004, 49(63: p. 253-258.
55. Bordeasu I, et al., Chemical and mechanical aspects of the cavitation phenomena, Revista De Chimie, 2007, 58(12): p. 1300-1304.
56. Ghiban B., et al., SOME ASPECTS OF CAVITATION DAMAGES IN AUSTENITIC STAINLESS STEELS, Annals of Daaam For 2008 & Proceedings of the 19th International Daaam Symposium, 2008: p. 541-542.
57. Bordeaşu I., G.B., Popoviciu M. O., Bălaşoiu V., Birău N., Karabenciov A., „The damage of austenite-ferrite steels by cavitation erosion", Annals of DAAAM for 2008 Proceedings of The 19th International DAAAM Symposium "Intelligent Manufacturing & Automation: Focus on New Generation of Intelligent Systems and Solutions", 2008: p. 0147-0148.
58. Bordeasu I., et al., CONTRIBUTIONS UPON THE CAVITATION EROSION OF TWO CAST IRONS USED IN MANUFACTURING CONTROL VALVES, Metalurgia International, 2009, 14(11): p. 5-7.
59. Bordeaşu I., P.M.O., Sălcianu L.C., Ghera C., Micu L.M., Bădărău R., Iosif A., Pirvulescu L.D., Podoleanu C.E., „A new concept for stainless steels ranking upon the resistance to cavitation erosion", International Conference on Applied Science, 2017, 163.
60. Ghiban B., et al., STRUCTURAL FEATURES OF CAVITATION DAMAGES IN SOME STAINLESS STEELS, Annals of Daaam For 2009 & Proceedings of the 20th International Daaam Symposium, 2009, 20: p. 1561-1562.
61. Ghiban N., et al., Evaluation of Mechanical Properties by Stereo-and Scanning Electron Microscopy of Some Heat Curing Dental Resins, Materiale Plastice, 2010, 47(2): p. 240-243.
62. Micu Lavinia Madalina, Comportarea la eroziune prin cavitatie a otelurilor inxidabile duplex, Teza de doctorat, Timisoara, 2017.
63. Karabenciov A,: „Cercetări asupra eroziunii produse prin cavitaţie vibratorie la oţelurile inoxidabile cu conţinut constant în nichel şi variabil de crom", Teza de doctorat, Timișoara, 2013.
64. Bordeasu I., Mitelea I:, Cavitation Erosion Behaviour of Stainless Steels with Constant Nickel and Variable Chromium Content, Materials Testing 54 (1), 53-58, 2012.
65. Mânzână M.E.: "Studii și cercetări experimentale privind modificările structurale produse prin cavitație-eroziune în diferite materiale metalice", Teza de doctorat, Bucuresti, 2012.
66. ***Standard method of vibratory cavitation erosion test, ASTM, Standard G32, 2016.
67. Bordeaşu I., Eroziunea cavitaţională asupra materialelor utilizate în construcţia maşinilor hidraulice şi elicelor navale, Efecte de scară,, Timişoara, 1997.
68. Tian N., Wang G., Zhou Y., Liu K., Zhao G., Zuo L., 2018 Study of the Portevin-Le Chatelier (PLC) Characteristics of a Al-Mg Aluminum Alloy Sheet in Two Heat Treatment States Materials 11. 1533; doi:10.3390/ma11091533
69. Franc Jean-Pierre, Jean-Louis Kueny, Ayat Karimi, Daniel-H, Fruman, Didier Fréchou, Laurence Briançon-Marjollet, Jean-Yves Billard, Brahim Belahadji, François Avellan, and Jean-Marie Michel, Cavitation, Physical mechanisms and industrial aspects, Grenoble, Presses Universitaires de Grenoble, 1995.
70. Steller Kazimir, Z. Reymann and T. Krzysztoowicz, "Evaluation of the resistance of materials to cavitational erosion," Proceedings of the Fifth Conference on Fluid Machinery, Vol 2, Akad Kiado, Budapest, 1975.

71. Pereira D., Oliveira J., Santos T., Miranda R., Lourenço F., Gumpinger J, and Bellarosa R, 2019 Aluminium to Carbon Fibre Reinforced Polymer tubes joints produced by magnetic pulse welding Compos, Struct, 230 pp 111512.
72. Manzana M. E. - Experimental studies and investigations regarding the structural modifications produced through cavitation-erosion in different metallic materials PhD Thesis, Universitatea Politehnica Bucuresti, 2012.
73. Guragata M.C.- Studies and experimental researches concerning plastic forming and erosion-cavitation behaviour of superalloy type INCONEL 718, PhD Thesis, Universitatea Politehnica Bucuresti, 2021
74. ***Standard method of vibratory cavitation erosion test, ASTM, Standard G32, 2016.
75. Bordeasu Ilare, Monografia Laboratorului de cercetare a eroziunii prin cavitaţie al Universităţii Politehnica Timişoara: (1960-2020)/Monograph of the Cavitation Erosion Research Laboratory of the Polytechnic University of Timisoara (1960-2020), Timisoara, POLITEHNICA Publishing House, 2020.
76. Micu Lavinia Madalina, Comportarea la eroziune prin cavitatie a otelurilor inoxidabile duplex/Cavitation erosion behavior of duplex stainless steels, Doctoral thesis, Timisoara, 2017.
77. Bordeasu Ilare and Ion Mitelea, "Cavitation Erosion Behavior of Stainless Steels with Constant Nickel and Variable Chromium Content," Materials Testing 54, no.1 (2012): 53-58.